

**SODIUM-GLUCOSE CO-TRANSPORTER 2 MEDIATES ANGIOTENSINOGEN
AUGMENTATION IN RENAL PROXIMAL TUBULAR CELLS UNDER HIGH
GLUCOSE CONDITIONS**

BY

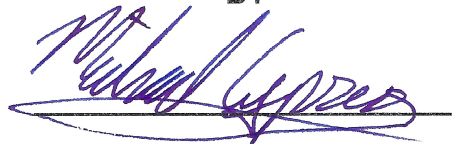
MICHAEL WINTHERS CYPRESS

Sodium-Glucose Co-Transporter 2 Mediates Angiotensinogen
Augmentation In Renal Proximal Tubular Cells Under High Glucose
Conditions

AN ABSTRACT

SUBMITTED ON THE TENTH DAY OF JULY 2017 TO THE GRADUATE
PROGRAM IN CELL & MOLECULAR BIOLOGY IN PARTIAL FULFILLMENT
OF THE REQUIREMENTS OF THE SCHOOL OF SCIENCE & ENGINEERING
OF TULANE UNIVERSITY FOR THE DEGREE OF DOCTOR OF PHILOSOPHY

BY



Michael W. Cypress

APPROVED:



L. Gabriel Navar, Ph.D. Director

Ryosuke Sato, Ph.D. Co-Director



Kenneth Mitchell, Ph.D.



Laura Schrader, Ph.D.



Ming Li, Ph.D.

ABSTRACT

Increased activity of the intrarenal renin-angiotensin system (RAS), in which proximal tubular angiotensinogen (AGT) is a key factor, has been implicated in the progression of diabetic nephropathy. AGT expression is upregulated in renal proximal tubular cells (PTC) by high glucose due to elevated reactive oxygen species (ROS) generation. Angiotensin II (Ang II) also promotes ROS generation. Glucose reabsorption in PTC occurs mainly through sodium-glucose co-transporter 2 (SGLT2). This study was performed to demonstrate that SGLT2 mediates AGT augmentation in PTC under hyperglycemic conditions. Furthermore, the enhancing effect of Ang II was investigated. Established mouse PTC were treated with 5 (normal), 15, or 25 mM D-glucose or D-mannitol (osmotic control). Pyruvate was used to investigate the role of glycolysis on AGT regulation. Glycolytic activity was quantified using a Seahorse metabolic analyzer. Tempol, an antioxidant, was used to determine the role of ROS. SGLT2 expression was silenced using shRNA. PTC were treated with high glucose and 10^{-10} - 10^{-7} M Ang II or an Ang II receptor blocker. AGT protein levels were increased by 15 (4.4 ± 0.2 -fold over control) and 25 mM (4.6 ± 0.2 -fold) glucose. AGT mRNA was also augmented (31.1 ± 3.5 -fold) by 25 mM glucose, but not mannitol. AGT expression was stimulated by pyruvate (10.7 ± 1.0 -fold over control), and exposure to 10, 15, or 25 mM glucose increased glycolytic activity (3.10 ± 0.28 -fold, 2.74 ± 0.20 -fold, and 2.75 ± 0.34 -fold, respectively), suggesting that enhanced glycolysis stimulates AGT expression. ROS accumulation increased (3.03 ± 0.29 -fold) in 25 mM glucose over control. Tempol attenuated

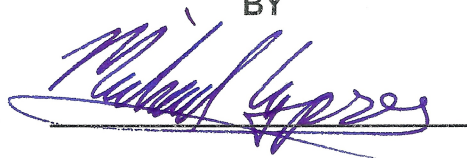
glucose-induced AGT augmentation by 77%, suggesting that ROS generation contributes to AGT upregulation. SGLT2 knockdown prevented AGT augmentation in 15 mM glucose, indicating that SGLT2 plays a key role mediating AGT upregulation by high glucose. Ang II receptor blockade did not alter AGT levels, and Ang II did not enhance AGT expression in normal or high glucose. Similarly, SGLT2 expression was unchanged by glucose or Ang II. These results indicate that SGLT2 contributes to AGT upregulation in PTC by high glucose, which helps to explain the mechanisms causing intrarenal RAS activation and consequent diabetic nephropathy.

Sodium-Glucose Co-Transporter 2 Mediates Angiotensinogen
Augmentation In Renal Proximal Tubular Cells Under High Glucose
Conditions

A DISSERTATION

SUBMITTED ON THE TENTH DAY OF JULY 2017 TO THE GRADUATE
PROGRAM IN CELL & MOLECULAR BIOLOGY IN PARTIAL FULFILLMENT
OF THE REQUIREMENTS OF THE SCHOOL OF SCIENCE & ENGINEERING
OF TULANE UNIVERSITY FOR THE DEGREE OF DOCTOR OF PHILOSOPHY

BY



Michael W. Cypress

APPROVED:



L. Gabriel Navar, Ph.D. Director



Ryosuke Sato, Ph.D. Co-Director



Kenneth Mitchell, Ph.D.



Laura Schrader, Ph.D.



Ming Li, Ph.D.

© Michael Cypress
All rights reserved
2017

ACKNOWLEDGEMENTS

To begin, I would like to thank my advisor, Dr. L. Gabriel Navar for his support over the past five years. The direction, guidance, and encouragement he has given me was vital to completing this project. His contribution to my scientific education has been immeasurable, and I have greatly benefitted from his wisdom and leadership. Working under such an eminent scientist has been a tremendous privilege, and I am grateful for the experience.

Next, I would also like to thank my supervisor Dr. Ryosuke Sato for his tremendous efforts and instruction. As I have developed my skills, his training has been immensely helpful, and I have learned countless valuable lessons from him. Dr. Sato has also shown me the importance of never being satisfied with my abilities and constantly striving to improve. I greatly appreciate all that he has done to help with the completion of this project and to share his expertise.

I sincerely thank the members of my committee, Dr. Kenneth Mitchell, Dr. Laura Schrader, and Dr. Ming Li, for the roles they have played in my graduate education. Their suggestions and advice have been crucial to my completion of this project. In addition, the courses I took from them – Renal Physiology, Systems Neuroscience, and Quantitative Physiology – were among the most rewarding and intellectually stimulating classes I've taken.

I would also like to acknowledge Dr. Ulrich Hopfer for generously providing the mouse proximal tubular cell line used in this study, Dr. T. Cooper Woods for helping to develop this project, Dr. Prasad Katakam for providing the use and

training of the Seahorse Extracellular Flux analyzer, and Dr. Zubaida Saifudeen for providing the use and training of the Neon Electroporation System. Their contributions greatly expanded the range of the experimental techniques available to me and made this project possible.

Ms. Akemi Katsurada and Dr. Kayoko Miyata taught me many experimental techniques and helped me solve problems that arose. Their advice and assistance was incredibly helpful and I greatly appreciate their help.

My friends at Tulane have been a great source of encouragement and reassurance. I would like to thank Ashley, Chase, Kate, and Felicia for countless memories. Special thanks goes to Catherine, who started the program at the same time as me. All of the challenges, struggles, and calamities that we've overcome would have been much harder to face alone.

I am deeply thankful for my friends from Rochester – Chris, Dan, and John – who have been in constant contact for the last seven years. They have played an integral role in my personal and professional development; one that would be difficult to articulate here. In addition, singular thanks goes to Matthew, who has been a friend, supporter, and confidant for over two decades. I would also like to acknowledge the outstanding teachers who helped foster my passion for science and mathematics, including Ms. Richardson, Mr. Schmidt, Dr. Funkenstein, Mr. Hoover-Dempsey, Mr. Flatau, and Dr. Brandt.

I am also thankful for my girlfriend Katrina, who has made finishing my Ph.D. much more bearable and far more meaningful. I am deeply grateful for the unwavering support she has given me.

The love and encouragement I have received from my family has been instrumental to all of my achievements. During grad school, my grandmother Bette, my aunt Cheryl and uncle Greg, and my sister Laura have been a constant source of positivity and motivation when I've needed it the most.

Finally, my deepest gratitude is reserved for my parents, Valerie and Larry Cypress, to whom this dissertation is dedicated. The endless love and support they have given me would be impossible to express, and I am eternally grateful for everything.

Funding for this study was provided by the following sources:

National Institutes of Health Center of Biomedical Research Excellence

(COBRE: P30GM103337)

National Institute of Diabetes and Digestive and Kidney Diseases

(Satou: R01DK107694; Cypress: F31DK107185)

American Heart Association Predoctoral Fellowship

(Cypress: 15PRE25090156)

TABLE OF CONTENTS

ACKNOWLEDGEMENTS	ii
LIST OF FIGURES	viii
LIST OF ABBREVIATIONS	x
CHAPTER 1 Introduction and Background	1
1.1 Renin-Angiotensin System	1
1.1.1 Overview of the renin-angiotensin system cascade	1
1.1.2 Systemic RAS regulation	2
1.2 Intrarenal RAS	4
1.2.1 Local versus systemic RAS activity	4
1.2.2 Intrarenal Ang II	5
1.2.3 Effects of Ang II on renal hemodynamics	7
1.2.4 Localization and origin of intrarenal AGT	7
1.2.5 Role of intrarenal AGT and Ang II	8
1.3 Renal Mechanisms of Glucose Homeostasis	9
1.3.1 Glucose reabsorption in the proximal tubule	9
1.4 Diabetic Nephropathy	15
1.4.1 Diabetes mellitus and the development of kidney injury	15
1.4.2 Intrarenal RAS and diabetic kidney injury	16
1.4.3 Mitochondrial ROS exacerbates PTC damage	18

1.4.4	AT1R-induced ROS generation	20
1.5	SGLT2 Blockade in the Management of Type 2 DM	20
1.5.1	History and development of SGLT2 inhibitors	21
1.5.2	Effects of SGLT2 inhibition on glucose reabsorption	21
1.5.3	Effects of SGLT2 on renal hemodynamics	23
1.5.4	Potential renoprotective effects of SGLT2 blockade	24
1.6	Unanswered Questions and Hypothesis	24
1.7	Thesis Aims	25
CHAPTER 2	Materials and Methods	28
2.1	Cell Line	28
2.2	Drugs	30
2.3	High Glucose Treatment	30
2.4	Quantitative Real-Time PCR	31
2.5	Western Blot Analysis	33
2.6	ROS Detection	33
2.7	Metabolic Activity Analysis	34
2.8	SGLT2 Gene Expression Knockdown	38
2.9	Electroporation	40
2.10	Statistical Analysis	41
CHAPTER 3	Specific Aim 1: Establish that SGLT2 mediates the upregulation of AGT in PTC under high glucose conditions by increasing glucose reabsorption and ROS generation	42
3.1	Research Design for Specific Aim 1	42

3.2	Results	43
3.2.1	AGT expression levels are increased by exposure to high glucose conditions.....	43
3.2.2	AGT is augmented by increased glucose metabolism	47
3.2.3	Increased ROS generation mediates glucose-induced AGT expression in mPTC	50
3.2.4	SGLT2 mediates glucose-induced AGT upregulation	53
CHAPTER 4	Specific Aim 2: Demonstrate that AT1R activation enhances the upregulation of AGT expression and ROS generation under high glucose conditions in PTC	55
4.1	Research Design for Specific Aim 2	55
4.2	Results	55
4.2.1	AT1R activation does not enhance high glucose-induced AGT upregulation	55
4.2.2	SGLT2 expression is not enhanced by high glucose or Ang II treatment	57
CHAPTER 5	Discussion and Conclusions	61
CHAPTER 6	List of References	72

LIST OF FIGURES

Figure 1.1.1 Overview of the RAS cascade.

Figure 1.2.1 Localization of intrarenal RAS components.

Figure 1.3.1 Glucose transport characteristics in different proximal tubular segments.

Figure 1.3.2 Model of sodium-glucose co-transport.

Figure 1.3.3 Glucose transporters in the proximal tubule.

Figure 1.4.1 AGT expression is upregulated during type 1 DM as a consequence of ROS generation.

Figure 1.4.2 ROS generation in the mitochondrial ETC.

Figure 1.5.1 Effects of SGLT2 inhibition on renal glucose reabsorption and blood pressure.

Figure 1.7.1 Proposed model of AGT upregulation by high glucose in proximal tubular cells.

Figure 2.1 mPTC culture.

Figure 2.4 Overview of qPCR.

Figure 2.6 ROS detection using H₂DCF-DA.

Figure 2.7 Metabolic analysis using extracellular flux.

Figure 2.8 Vector map of the plasmid containing the shRNA sequence targeting SGLT2.

- Figure 3.1** High glucose exposure stimulates AGT expression in mPTC.
- Figure 3.2** High glucose exposure induces glycolytic activity in PTC.
- Figure 3.3** AGT expression is stimulated by pyruvate.
- Figure 3.4** High glucose treatment promotes ROS accumulation.
- Figure 3.5** ROS generation is required for AGT augmentation under high glucose conditions.
- Figure 3.6** SGLT2 mediates glucose-induced AGT augmentation.
- Figure 4.1** AT1R activation is not required for AGT upregulation by high glucose.
- Figure 4.2** Ang II does not enhance glucose-induced AGT augmentation.
- Figure 4.3** SGLT2 protein levels are not enhanced by high glucose or Ang II.

LIST OF ABBREVIATIONS

ACE – angiotensin converting enzyme

AGT – angiotensinogen

Ang II – angiotensin II

ANOVA – analysis of variance

ARB – angiotensin receptor blocker

AT1R – angiotensin II type 1 receptor

ATP – adenosine triphosphate

DM – diabetes mellitus

ECAR – extracellular acidification rate

GAPDH – glyceraldehyde 3-phosphate dehydrogenase

GLUT – glucose transporter

GSC – glomerular sieving coefficient

H₂DCF-DA – 2',7'-dichlorodihydrofluorescein diacetate

GFR – glomerular filtration rate

JG – juxtaglomerular cells

NADH – nicotinamide adenine dinucleotide

NADPH – nicotinamide adenine dinucleotide phosphate

PTC – proximal tubular cell

RAS – renin-angiotensin system

RBF – renal blood flow

ROS – reactive oxygen species

RT-PCR – reverse transcription polymerase chain reaction

SGLT1 – sodium glucose cotransporter 1

SGLT2 – sodium glucose cotransporter 2

shRNA – short hairpin RNA

STZ – streptozotocin

TEMPOL – 4'-Hydroxy-TEMPO

CHAPTER 1 – INTRODUCTION AND BACKGROUND

1.1 Renin-Angiotensin System

1.1.1 Overview of the renin-angiotensin system cascade

The renin-angiotensin system (RAS) is a hormone system involved in the regulation of blood pressure and body fluid volume. In the classical RAS cascade, the enzyme renin, which is the rate-limiting enzyme in RAS, is secreted from the renal juxtaglomerular (JG) cells into the circulation and renal interstitial fluid. Renin binds to angiotensinogen (AGT), the precursor protein for angiotensin peptides and the only known substrate for renin ¹. Renin cleaves the N-terminus of AGT to produce the decapeptide angiotensin I (Ang I). While Ang I has no biological functions, it is converted into several bioactive peptides ². Angiotensin II (Ang II) is the most important RAS hormone. It is primarily formed by angiotensin-converting enzyme (ACE) ³, but it can also be generated by other peptidases, such as chymase ⁴.

Ang II exerts its physiological effects through activation of the Ang II receptors. The well-characterized receptors are the Ang II type 1 receptor (AT1R) and Ang II type 2 receptor (AT2R). AT1R and AT2R are both G-protein coupled receptors found in many different cell types ^{1, 5}. AT1R is the main receptor responsible for the physiological effects of Ang II. In general, AT2R produces the

opposite effects of AT1R activation ⁶. AT2R has also been shown to play a major role in fetal development ⁷.

Upon Ang II binding, AT1R stimulates downstream molecular pathways by activating G α and phospholipase C. Consequently, this causes an increase in inositol 1,4,5-triphosphate and intracellular calcium signaling, resulting in protein kinase C activation ⁸. AT1R activation initiates several different physiological responses that act in concert to promote sodium and water retention and increased arterial blood pressure. On blood vessels, AT1R induces contraction in vascular smooth muscle cells, causing vasoconstriction ⁹. In the proximal tubules, AT1R promotes sodium and water reabsorption by enhancing Na⁺/H⁺ Exchanger activity in the proximal tubule ¹⁰. AT1R can also directly stimulate sodium reabsorption in the collecting duct by enhancing epithelial sodium channel activity ¹¹. AT1R stimulates aldosterone secretion from the adrenal gland, causing increased sodium reabsorption in the distal tubules and collecting duct ¹² (Fig. 1.1.1).

1.1.2 Systemic RAS regulation

Renin release from JG cells can be triggered by a drop in pressure in the afferent arteriole ¹³, decreased salt delivery to the macula densa ¹⁴, or sympathetic nervous system activation ¹⁵. Studies in human and animal models have demonstrated that renin secretion is inhibited by Ang II ^{16, 17}. Circulating AGT is predominantly synthesized in the liver and released into the blood stream. In humans, plasma concentrations of AGT are much higher than renin

FIGURE 1.1.1

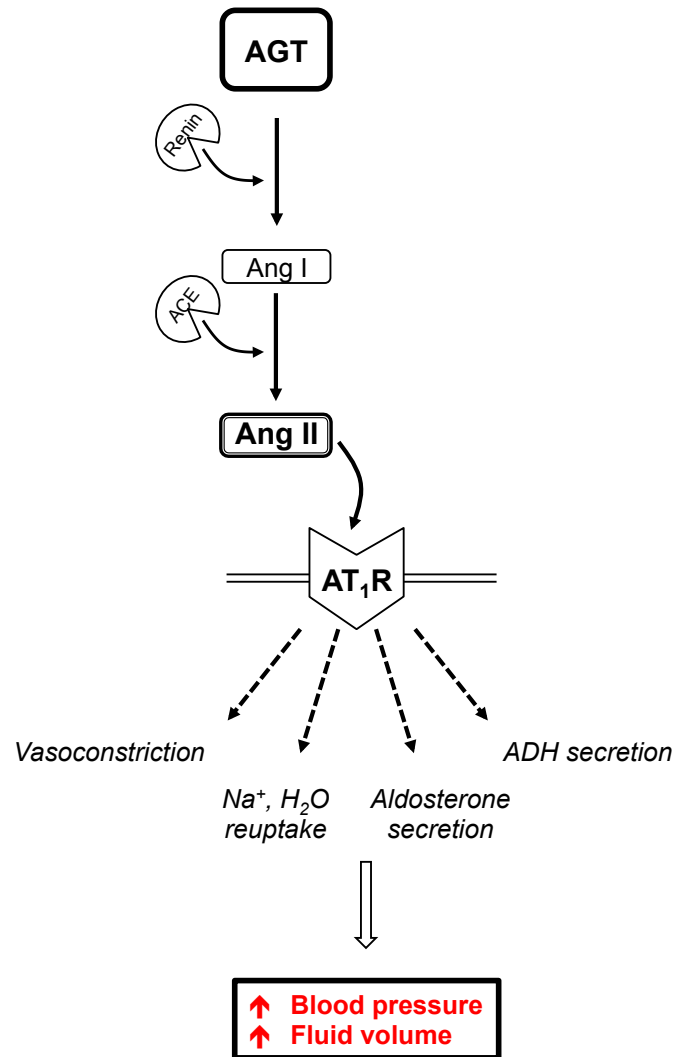


Figure 1.1.1: Overview of the RAS cascade. Renin cleaves AGT to form Ang I, which is converted to Ang II by ACE. Ang II binds to AT₁R, leading to an increase in arterial pressure and fluid volume.

concentrations ¹⁸, suggesting that renin secretion is the rate-limiting step influencing Ang II formation.

However, in humans, plasma AGT concentrations are similar to the Michaelis-Menton constant (K_m) for renin ^{19, 20}, suggesting that changes to plasma AGT can also influence the reaction rate. There is evidence that injection of AGT induces an increase in blood pressure in rats on a low-salt diet ²¹. Moreover, an epidemiological survey found a strong correlation between plasma AGT levels and blood pressure ²², and polymorphisms of the AGT promoter region are associated with hypertension and influence AGT transcription ^{18, 23}. Therefore, AGT regulation can also influence circulating Ang II levels ²⁴.

1.2 Intrarenal RAS

1.2.1 Local versus systemic RAS

RAS activation was primarily characterized as an endocrine system, and most research focused on the systemic effects of circulating Ang II. However, the existence of local RAS activity has been discovered in several organs including the brain ²⁵, heart ²⁶, adipose tissue ²⁷, and kidneys ^{28, 29}. In particular, tissue-specific RAS activity has been well-described in the kidneys, and is regulated independently of the circulating RAS ³.

AT1R is expressed along the nephron ⁵, indicating that intratubular Ang II plays a physiological role. Also, a study using mice with targeted disruption of the *Agtr1a* gene observed the effects of kidney cross-plantation in wild-type and AT1_AR knockout mice. They found that chronic Ang II infusion promoted

hypertension in wild-type and systemic AT₁R KO mice, but not in total AT₁R KO mice or kidney-specific AT₁R KO mice³⁰. This suggests that kidney-specific AT₁R activation mediates the pathogenesis of Ang II-dependent hypertension.

1.2.2 Intrarenal Ang II

Ang II levels in the kidney can be derived from systemic and locally generated Ang II^{3, 31}. However, analysis of the renal tubular fluid has shown that Ang II and AGT concentrations are much higher than in the plasma^{31, 32}, and Ang II is secreted by the proximal tubule³³. Moreover, renin is secreted from JG cells into the renal interstitium³⁴ and the proximal tubule³⁵. AGT is found in the proximal tubule²⁹. ACE is present on the luminal membrane throughout the rat nephron³⁶, and systemic Ang I infusion can be converted into Ang II in the kidney^{37, 38}. Taken together, this suggests that all necessary RAS components are expressed in the kidney, and that intrarenal Ang II is largely comprised of locally formed peptides (Fig. 1.2.1).

Ang II internalization has also been shown to affect renal Ang II levels. In a study using salt-restricted rats, Ang I and Ang II levels in the plasma and renal cortex were enhanced compared to rats on a normal-salt diet, but the magnitude of this increase was higher in the kidney compared to the plasma³⁹. Furthermore, Ang II levels were increased more than Ang I. While AT₁R blockade increased plasma Ang II levels, cortical Ang II levels decreased³⁹. Ang II is internalized into proximal tubular cells (PTC), but losartan inhibits this effect⁴⁰. This suggests that Ang II internalization via AT₁R-mediated endocytosis contributes to intrarenal Ang II levels in response to a low-salt diet.

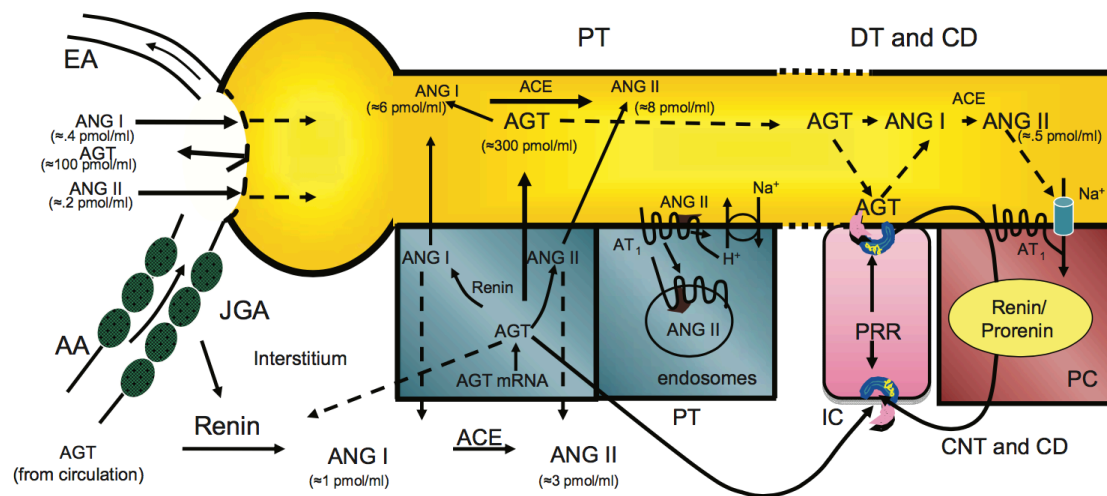
FIGURE 1.2.1

Figure 1.2.1: Localization of intrarenal RAS Components. The kidney produces all of the components required for local RAS activation. Concentrations of AGT and Ang II are much higher in the proximal tubule than plasma levels, suggesting that intrarenal Ang II is locally generated. AT₁R is found along the nephron, indicating that intrarenal Ang II has a physiological role ⁴¹.

1.2.3 Effects of Ang II on renal hemodynamics

Ang II constricts the renal afferent and efferent arterioles which increases vascular resistance, decreases renal blood flow, and increases filtration fraction^{37, 42}. Ang II also induces contraction of the mesangial cells, which reduces GFR by decreasing the glomerular filtration coefficient⁴³. Infusion of intratubular Ang II increases the sensitivity of the tubuloglomerular feedback mechanism³³. Taken together, these findings demonstrate that Ang II influences renal function by decreasing renal blood flow and GFR, and modulating the reabsorption of sodium and water in the kidney.

1.2.4 Localization and origin of intrarenal AGT

In the kidneys, *in situ* hybridization studies have demonstrated that AGT is expressed in rat²⁹ and mouse⁴⁴ PTC. AGT expression varies within different segments of the proximal tubule. While AGT protein is found in the S1 segment, basal AGT mRNA levels are very low, and relatively high in the S2 and S3 segments^{45, 46}. AGT protein is localized along the apical membrane^{44, 45} and is internalized from the tubular fluid via megalin^{45, 47}.

Normally, it is expected that AGT is too large to pass through the glomerular filter in the absence of kidney damage. Infused human AGT in rats was not detectable in the urine⁴⁸. In addition, a study of the glomerular permeability of AGT in mice by measuring the glomerular sieving coefficient (GSC) revealed very low permeability ($GSC < 0.001$) under normal conditions, and slightly elevated permeability during glomerular sclerosis ($GSC < 0.01$)⁴⁹. However, this point is still debated. A study utilizing mice with organ-specific AGT

gene knockouts demonstrated that liver-specific AGT knockout caused a significant decrease in renal AGT and Ang II. Conversely, AGT knockout in the kidney decreased urinary AGT, but had no effect on intrarenal AGT protein levels. This suggests that intrarenal AGT protein is derived from the plasma, while urinary AGT originates from the proximal tubule ⁴⁷.

Notwithstanding, another recent report demonstrated that nephron-specific AGT knockout reduced intrarenal AGT protein and mRNA and caused an unexpected reduction in plasma AGT levels ⁵⁰. Thus, the role of AGT synthesis in the proximal tubule has not been well-characterized. Basolateral transcytosis of AGT across PTC has also been reported, which could contribute to the high levels of AGT protein in the proximal tubule ⁴⁵, but the role is unclear, especially given the relatively high levels of AGT in the tubule compared to the plasma. Thus, the origin and function of AGT in the proximal tubule remains controversial and not entirely explained.

1.2.5 Role of Intrarenal AGT and Ang II in Hypertension

Intrarenal and urinary AGT levels are enhanced in salt-sensitive hypertensive rats ⁵¹ and models of Ang II-dependent hypertension in rats ^{48, 52-54} and mice ⁵³. In addition, ACE inhibition ⁵³ and AT1R blockers (ARB) ⁵⁴ attenuate the increase in AGT expression, indicating that AT1R activation contributes to AGT augmentation.

AGT synthesized in PTC is secreted into the tubule and excreted in the urine ⁴⁸. Renin is found in the collecting duct ⁴⁴, which suggests that secreted AGT can play a role in the distal nephron. Evidence for a functional role for

intrarenal AGT has been shown using transgenic mice developed to express human AGT in the proximal tubule. Overexpression of AGT in the proximal tubules promotes the development of hypertension in mice ⁵⁵⁻⁵⁸ which was independent of plasma Ang II levels. Moreover, RAS blockade attenuated this effect ⁵⁶. Taken together, this suggests that intrarenal AGT and Ang II have reciprocal regulation and can create an amplification feedback mechanism resulting in hypertension.

1.3 Renal Mechanisms of Glucose Homeostasis

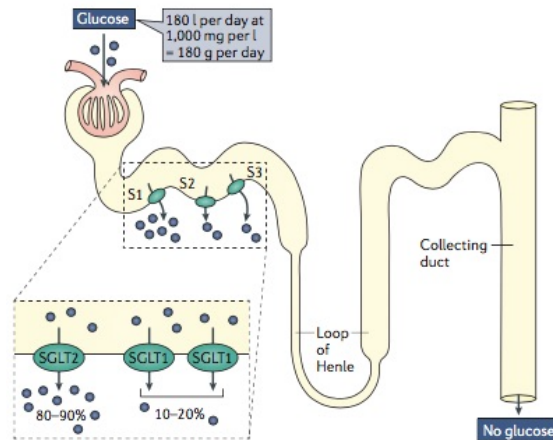
The kidneys play a key role in glucose processing through the filtration and reabsorption of plasma glucose ⁵⁹. In addition, the kidneys are capable of gluconeogenesis and are tied with the heart in having the highest metabolic rate of any major organ tissue, relative to mass, meaning they utilize significant amounts of glucose ^{59, 60}.

1.3.1 Glucose reabsorption in the proximal tubule

In healthy individuals, approximately 150 to 180 g of glucose are filtered per day and less than 500 mg are excreted in the urine ^{61, 62}. Micropuncture studies in mice ⁶³, rats ^{64, 65}, and rabbits ⁶⁶ have shown that the reabsorption of filtered glucose occurs almost entirely in the proximal tubule. The maximal glucose transport rate and glucose affinity vary significantly among the different segments of the proximal tubule ⁶⁷ (Fig. 1.3.1). The S1 segment has the highest reabsorption capacity and lowest glucose affinity ^{66, 68}, and it is responsible for the most glucose reabsorption under normal physiological conditions.

FIGURE 1.3.1

A



B

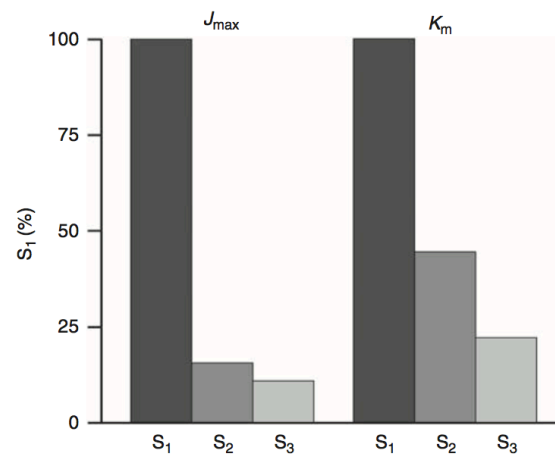


Figure 1.3.1: Glucose transport characteristics in different proximal tubular segments. (A) Illustration of glucose reabsorption in the nephron. The majority of glucose is reabsorbed in the S1 segment. The remaining glucose is scavenged in the S2 and S3 segments ⁶⁹. (B) J_{max} : maximum glucose transport rate. K_m : glucose affinity constant. Values are presented as a percentage of S1 ⁵⁹.

Conversely, the S2 and S3 segments have a high glucose affinity, but low capacity^{59, 61}. Renal glucose reabsorption occurs by removing glucose from the tubular fluid and returning it to the interstitial space. Glucose in the lumen must be transported into the PTC up its concentration gradient, and then return to the interstitial fluid down its concentration gradient. Thus, an active transport mechanism is needed to reabsorb glucose across the apical membrane. This is accomplished by coupling the entry of glucose to sodium, which moves down its concentration gradient^{70, 71} (Fig. 1.3.2). The two main transporters responsible for apical glucose reabsorption in the proximal tubule are sodium glucose co-transporters 2 and 1 (SGLT2 and SGLT1)^{63, 70, 72} (Fig. 1.3.3). The sodium gradient is maintained by Na⁺/K⁺-ATPase activity on the basolateral membrane of PTC⁷³.

SGLT2 is a transmembrane protein encoded by the *SLC5A2* gene. It is characterized as a low-affinity, high capacity glucose transporter that couples the reabsorption of sodium and glucose at a 1:1 ratio. In the kidneys, SGLT2 is expressed on the brush-border membrane of the S1 and S2 proximal tubular segments. Micropuncture experiments in mice lacking SGLT2 expression have demonstrated that SGLT2 is the main transporter responsible for glucose reabsorption in early PTC, suggesting that SGLT2-mediated glucose transport is the primary mechanism responsible for renal glucose reabsorption⁶³. In wild-type mice, approximately 80% of filtered glucose was reabsorbed in the early proximal tubular segments. In contrast, glucose reabsorption was almost entirely absent in the early proximal tubule of SGLT2^{-/-} mice. Moreover, glycosuria was observed in

FIGURE 1.3.2

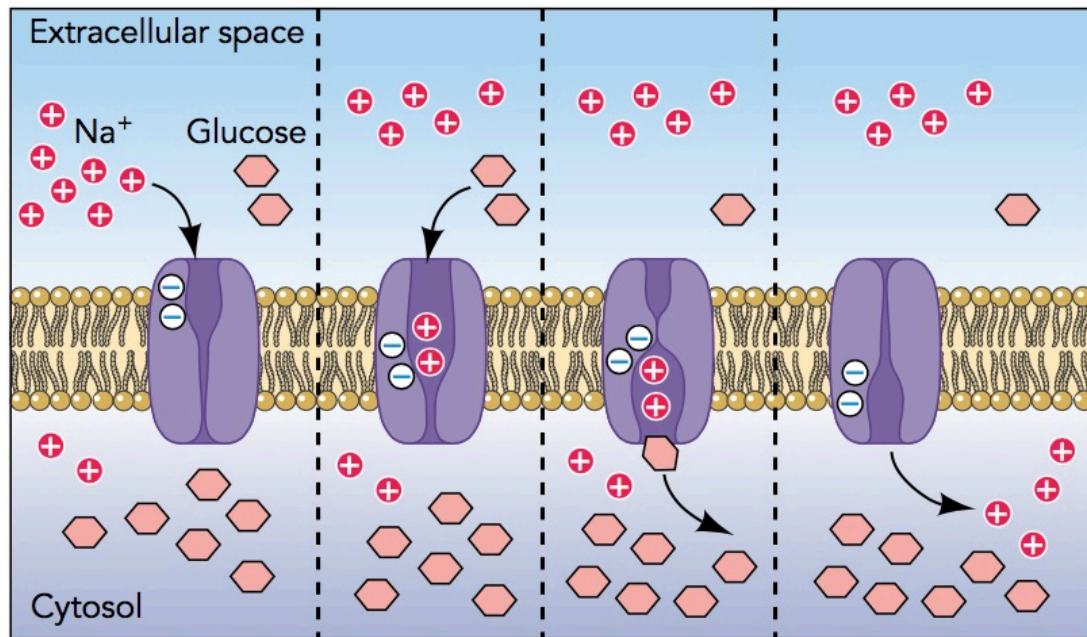


Figure 1.3.2: Model of sodium-glucose co-transport. Sodium binding induces a conformational change in the SGLT protein and exposes a glucose binding site. Sodium is transported down its concentration gradient, providing the energy for glucose to move up its concentration gradient ⁷⁴.

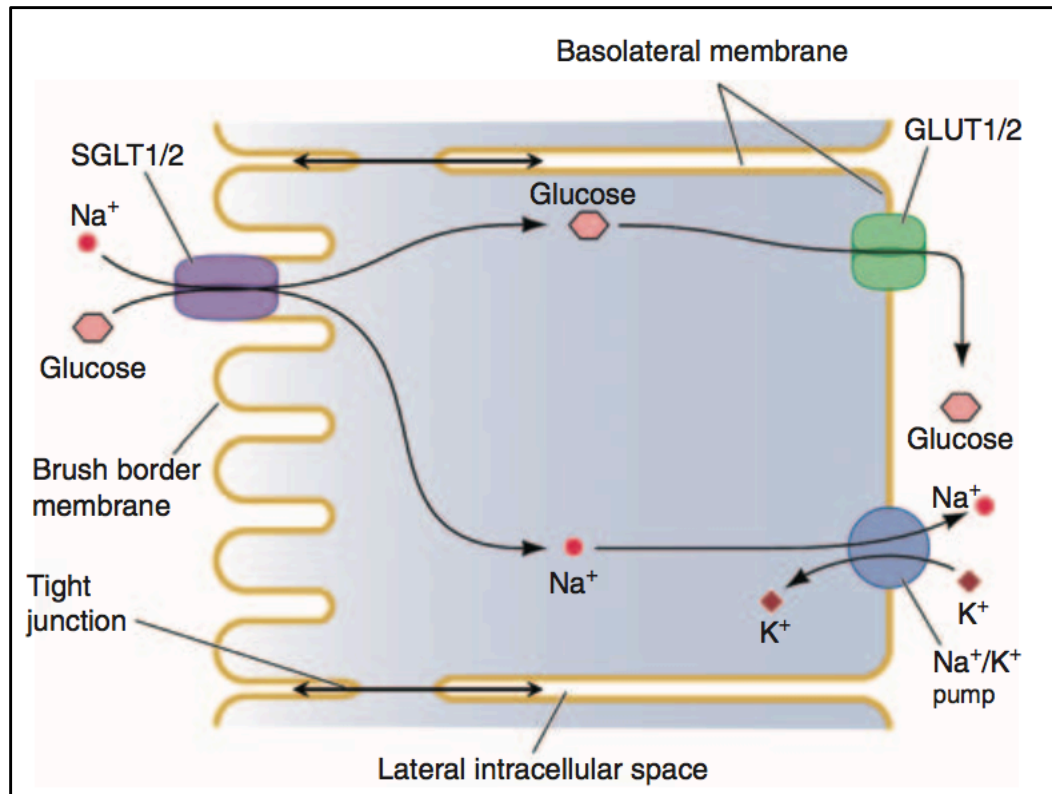
FIGURE 1.3.3

Figure 1.3.3: Glucose transporters in the proximal tubule. In the proximal tubule, apical glucose reabsorption is mediated by sodium-glucose co-transport. Glucose diffuses out of the cell via facilitative GLUT transporters on the basolateral membrane. Na⁺/K⁺-ATPase activity is responsible for maintaining the sodium gradient across the cell ⁵⁹.

SGLT2^{-/-} mice, despite the fact that plasma glucose levels and GFR were similar to wild-type mice. These findings are consistent with the phenotype found in familial renal glycosuria, an inherited disease characterized by loss-of-function mutations to SGLT2, where glucose excretion is present as a result of decreased proximal glucose reabsorption despite normal plasma glucose levels ⁷⁵.

SGLT1 is a high-affinity, low capacity glucose transporter that transports two molecules of sodium for each molecule of glucose. In the kidneys, SGLT1 is predominantly expressed in the S3 segment of the proximal tubule where it is responsible for reabsorbing the remaining glucose from the tubular fluid ^{69, 70, 76}. Because SGLT1 has a relatively high affinity for glucose, it serves as a useful counterpart to SGLT2, and is well-suited to scavenge the remaining glucose from the tubular fluid, where glucose concentrations are low ⁵⁹. SGLT1 also plays an important role in intestinal glucose reabsorption, and is expressed heavily on the brush border membrane of the small intestine ⁷⁶. SGLT1 expression has also been detected in other organs, including the lung, heart, and liver ⁷⁷.

The active transport mechanism of SGLT2/1 increases the intracellular glucose concentration relative to the interstitial fluid. This allows glucose to exit the PTC by passive diffusion through facilitative glucose transporters located on the basolateral membrane. Glucose transporter 2 (GLUT2), a high-capacity/low-affinity transporter, is the primary basolateral transporter in the early tubule ⁷⁸. There is also evidence that GLUT2 is translocated to the apical membrane during diabetes mellitus, which contributes to increased glucose reabsorption ^{79, 80}.

Glucose transporter 1 (GLUT1), a low-capacity/high-affinity transporter, is expressed in the late proximal tubules as a counterpart to SGLT1^{71, 78}.

1.4 Diabetic Nephropathy

1.4.1 Diabetes mellitus and the development of kidney injury

Diabetes mellitus (DM) is a metabolic disease causing chronically high blood glucose levels, and affects millions of people worldwide^{81, 82}. DM is a major risk factor for chronic kidney disease (CKD) in the United States, and affects nearly 40% of individuals with CKD⁸³. It is estimated that 30% of patients diagnosed with DM will develop diabetic nephropathy^{84, 85}, which is characterized by mesangial expansion, thickening of the glomerular basement membrane, glomerular sclerosis, and microalbuminuria^{84, 86}. This progresses into macroalbuminuria and kidney failure^{86, 87}.

Glomerular hyperfiltration⁸⁸ and renal hypertrophy^{89, 90} are risk factors for developing diabetic nephropathy. Micropuncture studies have shown that increased luminal glucose concentrations stimulate sodium reabsorption⁹¹, and concentrations of sodium, chloride, and potassium are decreased in the early distal tubular fluid in type 1 DM rats, while single nephron GFR (SNGFR) is increased⁹². SGLT2 upregulation has been reported in type 1⁹³ and type 2 DM rats⁹⁴, as well as in humans with type 2 DM⁹⁵. However, there are also conflicting studies where SGLT2 expression is decreased^{96, 97} or unchanged^{98, 99} in DM. In addition, SGLT2 downregulation under high glucose conditions has also been reported in rabbit PTC¹⁰⁰.

1.4.2 Intrarenal RAS and diabetic kidney injury

Increased activation of the intrarenal RAS has been proposed as a key factor in the progression of diabetic nephropathy. Clinical reports demonstrate that RAS blockade attenuates the progression of diabetic nephropathy in type 1¹⁰¹ and type 2 DM^{102, 103}. There is also evidence that Ang II blockers prevent DM-associated increase in urinary AGT and markers of oxidative stress¹⁰⁴. Studies in mouse PTC have demonstrated that AT1R activation enhances transforming growth factor- β 1 (TGF- β_1) expression and promotes cellular hypertrophy^{105, 106} and apoptosis¹⁰⁷. In addition, RAS blockade attenuated TGF- β_1 upregulation, apoptosis, and tubular fibrosis in hypertensive rats with STZ-induced DM¹⁰⁸, suggesting that intrarenal RAS activation contributes to increased apoptosis in PTC in DM.

While intrarenal RAS activation is not universally observed in DM¹⁰⁹, increased levels of cortical intrarenal AGT and Ang II have been reported in type 2 DM rats before the onset of renal injury^{110, 111}. AT1R blockade has been shown to attenuate the increased AGT and Ang II levels¹¹¹. Several recent studies provide evidence that AGT upregulation contributes to the pathogenesis of diabetic nephropathy. Urinary AGT levels are enhanced in humans¹¹² and in animal models of type 1 DM¹¹³ (Fig. 1.4.1). Moreover, enhanced AGT is observed prior to the development of microalbuminuria, suggesting that intrarenal AGT expression is upregulated in the early stages of DM. Similar results were found in another report which also investigated the role of oxidative damage in the upregulation of intrarenal AGT using a transgenic mouse model that

FIGURE 1.4.1

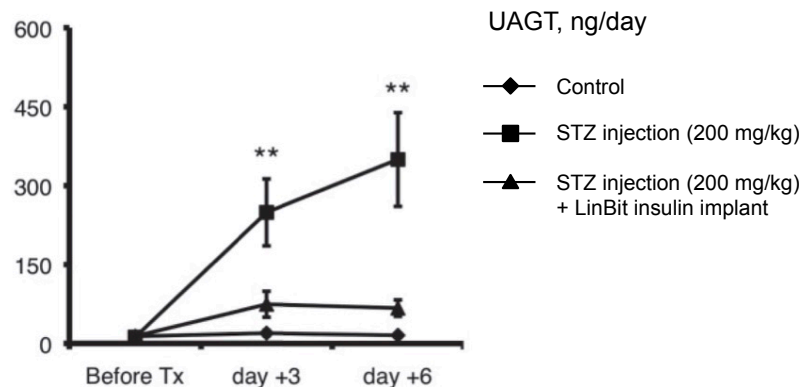
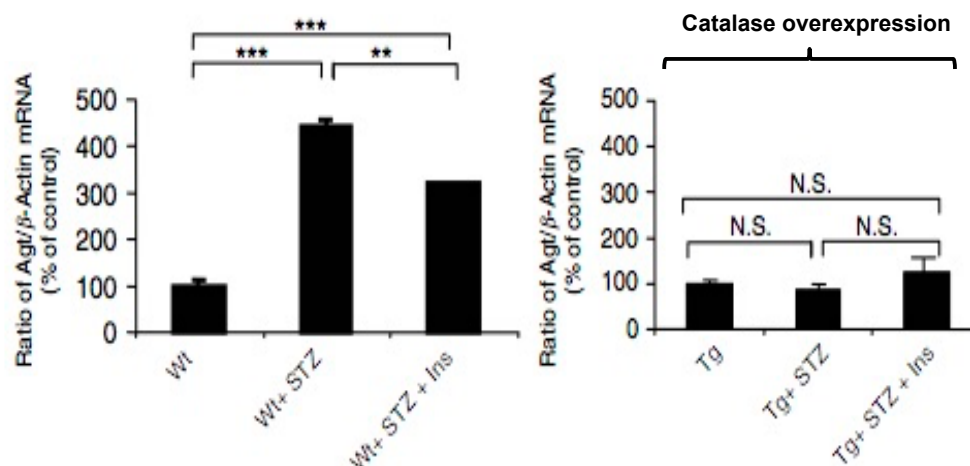
A**B**

Figure 1.4.1: AGT expression is upregulated during type 1 DM as a consequence of ROS generation. (A) Urinary AGT levels are increased during STZ-diabetic mice¹¹³. (B) AGT mRNA levels are increased in the proximal tubules of STZ-diabetic mice. However, catalase overexpression in PTC prevents this increase, suggesting that ROS generation plays a crucial role in glucose-induced AGT upregulation¹¹⁴.

overexpresses catalase in the proximal tubule, preventing ROS generation. In wild-type mice, STZ-induced diabetes led to an increase in AGT mRNA levels in PTC, but the transgenic mice showed no increase in AGT expression. This suggests that ROS contributes to the stimulation of AGT during diabetes ¹¹⁴.

Exposure to high glucose directly stimulates AGT expression levels in cultured PTC and is blocked by inhibition of the mitochondrial electron transport chain, indicating that AGT is upregulated by increased glucose metabolism and cellular respiration ^{115, 116}. Taken together, these results demonstrate that AGT upregulation in the proximal tubule plays a key role in the development and progression of diabetic nephropathy.

1.4.3 Mitochondrial ROS exacerbates PTC damage

The mitochondrial matrix is a major site of ROS generation. Specifically, nicotinamide adenine dinucleotide (NADH) dehydrogenase and the cytochrome *bc*₁ complex promote the formation of superoxide ($O_2^{\cdot-}$) as a by-product of glucose metabolism ¹¹⁷⁻¹¹⁹ (Fig. 1.4.2). During oxidative phosphorylation, NADH oxidation provides the energy required to facilitate the transfer of protons from the mitochondrial matrix to the inner membrane space. However, because this process is not entirely efficient, oxygen can also act as an electron acceptor, resulting in occasional superoxide formation during glucose metabolism ¹¹⁹.

While $O_2^{\cdot-}$ is produced under normal conditions, a study in rat PTC found that exposure to 25 mM glucose generated an increase in ATP levels and $O_2^{\cdot-}$ generation, leading to a loss of cell viability and cytochrome *bc*₁ complex inactivation. These effects were mitigated by manganese superoxide dismutase,

FIGURE 1.4.2

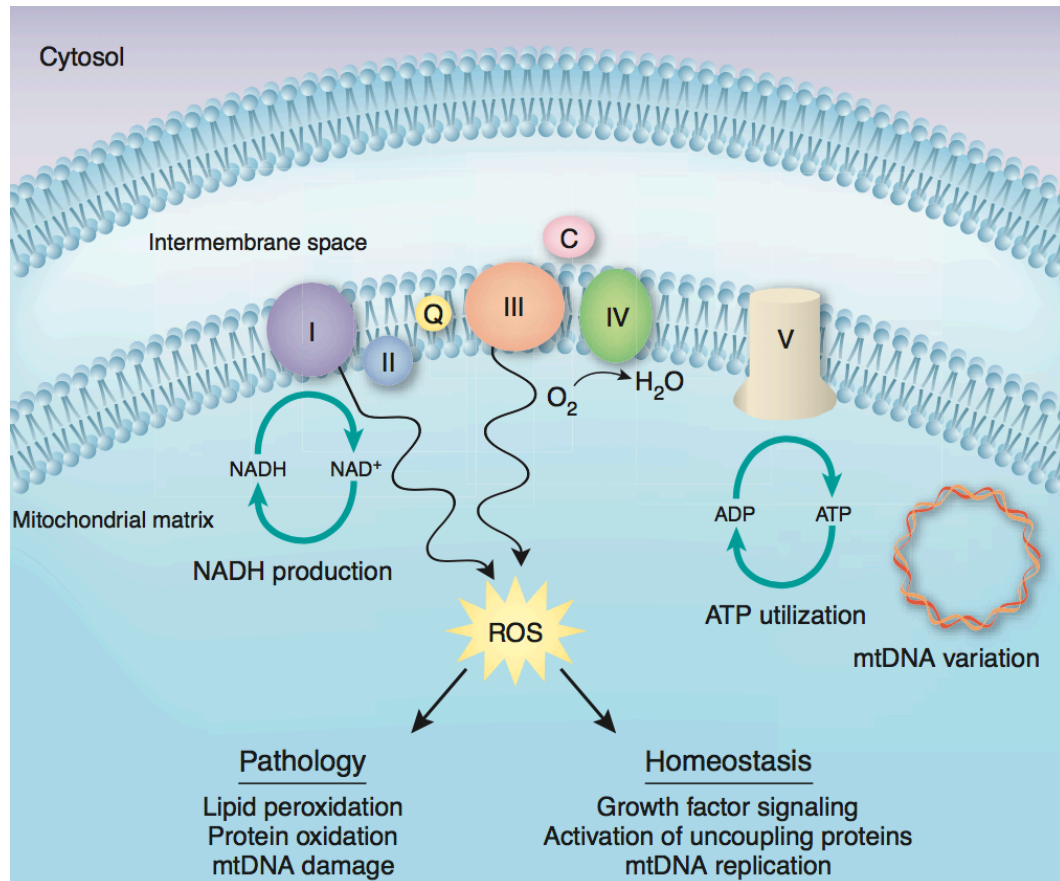


Figure 1.4.2: ROS generation in the mitochondrial ETC. Mitochondrial ROS generation occurs as a result of oxidative phosphorylation in the electron transport chain. The reactions involving NADH dehydrogenase (I) and the cytochrome *bc*₁ complex (III) are not entirely efficient, and occasionally result in the transfer of electrons to oxygen, producing O₂^{•-} ¹²⁰.

suggesting that the accumulation of mitochondrial $O_2^{\cdot-}$ contributes to glucose-induced mitochondrial dysfunction in PTC ¹²¹.

1.4.4 AT1R-induced ROS generation

AT1R activation also promotes the formation of ROS generation by stimulating NADPH oxidase activity ¹²². Ang II treatment (10^{-7} M) induced an increase in $O_2^{\cdot-}$ generation in cultured PTC from both mouse and porcine kidneys ¹²³. Treatment with 4-Hydroxy-TEMPO (tempol), an antioxidant, prevented the augmentation of intrarenal AGT levels in salt-sensitive hypertensive rats ¹²⁴. In mice, transgenic overexpression of AGT in PTC resulted in elevated ROS generation compared to wild-type, and was attenuated by apocynin, an NADPH oxidase inhibitor ¹²⁵. Apocynin also reversed albuminuria, apoptosis, and tubulointerstitial fibrosis in transgenic mice, suggesting that ROS generation contributes to RAS-associated renal injury.

1.5 SGLT2 Blockade in the Management of Type 2 DM

A new class of drugs targeting SGLT2 has been approved for the treatment of hyperglycemia during type 2 DM. SGLT2 inhibitors block the reabsorption of filtered glucose by competitively binding to SGLT2, causing glycosuria ¹²⁶. In patients with uncontrolled type 2 DM with HbA_{1c} levels above 8.0%, treatment with SGLT2 inhibitors leads to decreased total HbA_{1c} levels by approximately 0.8% from the starting point, indicating a reduction in plasma glucose levels ¹²⁷. Studies have also observed enhanced insulin sensitivity,

reduced blood pressure, and attenuated hyperfiltration in DM patients during SGLT2 inhibition¹²⁸⁻¹³⁰ (Fig. 1.5.1).

1.5.1 History and development of SGLT2 inhibitors

SGLT2 inhibitors are derivatives of the compound phlorizin, a naturally occurring compound found in certain species of apple trees¹³¹. Phlorizin is a glucoside which binds to SGLT2 and SGLT1, and prevents glucose entry by acting as a competitive inhibitor⁷⁰. Phlorizin has been used in research to study the mechanisms of renal transport by blocking the proximal reabsorption of glucose, sodium, and water^{132, 133}. Because it promotes glycosuria, it was investigated for its potential as a treatment for diabetes. However, because it also blocks SGLT1, it interfered with intestinal glucose reabsorption, causing gastrointestinal side effects¹²⁷.

The major drawback to phlorizin stems from the fact that the binding affinity for SGLT2 is approximately 6-fold higher than that for SGLT1, meaning it has relatively low selectivity for SGLT2⁷⁰. Accordingly, synthetic derivatives of phlorizin were developed to increase the selectivity for SGLT2. Modern SGLT2 inhibitors have a 300- to 1200-fold higher selectivity for SGLT2 compared to SGLT1^{134, 135}. This reduces the side effects associated with phlorizin, making the drugs more valuable as therapeutics.

1.5.2 Effects of SGLT2 inhibition on glucose reabsorption

In individuals with normal glucose tolerance, SGLT2 inhibitors cause a dose-dependent increase in glucose excretion, without causing hypoglycemia¹³⁶.

FIGURE 1.5.1

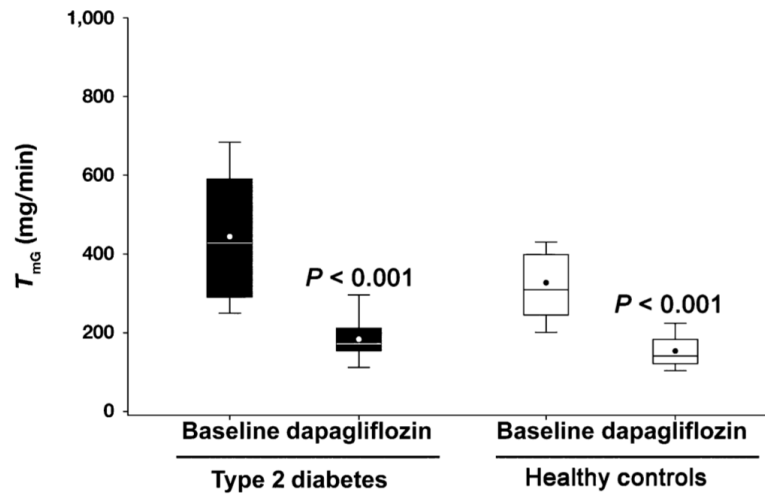
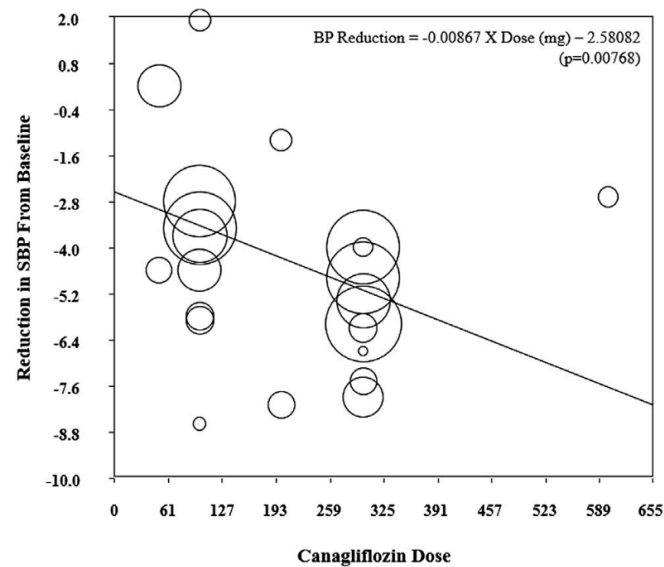
A**B**

Figure 1.5.1: Effects of SGLT2 inhibition on renal glucose reabsorption and blood pressure. (A) Maximum renal glucose reabsorption is reduced during SGLT2 inhibition in type 2 DM patients and healthy control subjects ¹³⁷. (B) A meta-analysis of clinical data during treatment with canagliflozin demonstrates a dose-dependent reduction in blood pressure ¹³⁸.

However, the maximum urinary glucose excretion achieved with high doses of SGLT2 inhibition is approximately 50-70 grams per day^{139, 140}, which represents approximately 30-50% of the total daily filtered glucose load in normal individuals (~180 g). This is somewhat counterintuitive considering the evidence that SGLT2 is responsible for >80% of glucose reabsorption⁶³.

One proposed explanation for this observation is that SGLT2 inhibition leads to an increase in glucose reabsorption in the late proximal tubule through SGLT1⁶¹. Under normal conditions, most glucose has been absorbed in the early tubule, therefore glucose reabsorption in the S3 segment is well under the maximum reabsorption rate. During SGLT2 inhibition, glucose load to the S3 segment is greatly increased, which causes SGLT1 to reabsorb glucose at full capacity. This is consistent with data in SGLT2 knockout mice and individuals with familial renal glycosuria^{63, 75}.

1.5.3 Effects of SGLT2 on renal hemodynamics.

Recent reports have demonstrated that SGLT2 inhibitors influence renal hemodynamics during DM by blocking the proximal reabsorption of sodium, causing an increase in sodium load to the macula densa. In STZ diabetic rats, SGLT2 inhibition led to TGF activation and single nephron GFR reduction. The hemodynamic effects were stronger during acute treatment, but TGF activation was still present during chronic SGLT2 inhibition¹⁴¹. Additionally, a study in type 1 DM patients found that SGLT2 inhibition caused a decrease in GFR and renal vascular resistance in patients with hyperfiltration over 8 week treatment. Diabetic patients without hyperfiltration showed no change in GFR¹³⁰. Moreover,

in this study, the effects on renal hemodynamics were measured in patients under euglycemic and hyperglycemic clamp. They found that GFR was lowered during SGLT2 inhibition in both conditions, suggesting that the decrease in hyperfiltration occurs independently of the blood glucose-lowering effects.

1.5.4 Potential renoprotective effects of SGLT2 blockade

In addition to normalizing HbA_{1c} levels, clinical studies and animal models of DM have shown potential beneficial side-effects from SGLT2 inhibitors that might improve treatment outcomes and prevent kidney disease independently of their capacity for lowering blood glucose ¹⁴². SGLT2 inhibitors are also associated with a modest, yet significant drop in blood pressure in type 2 DM patients ^{138, 143, 144}. Also, in type 2 DM mice ¹⁴⁵ and rats ¹⁴⁶, SGLT2 inhibition led to a decrease in proteinuria and glomerular damage. This suggests that SGLT2 inhibitors could play a role in the prevention of diabetic nephropathy.

1.6 Unanswered Questions and Hypotheses

While SGLT2 is the main transporter responsible for glucose reabsorption in PTC, and increased AGT expression is observed during hyperglycemia, the contribution of SGLT2-dependent glucose transport on AGT augmentation has not been established. Additionally, although high glucose and Ang II increase ROS, the effects of AT1R activation on glucose-induced ROS generation and AGT expression have not been well-characterized. Specifically, it is not known if Ang II treatment during high glucose exposure will have additive or synergistic effects on AGT expression.

Therefore, we hypothesized that increased SGLT2-mediated glucose transport promotes ROS generation and consequent AGT upregulation in PTC under hyperglycemic conditions. Furthermore, Ang II will intensify the stimulation of AGT expression under high glucose conditions by AT1R activation and consequent ROS generation. Accordingly, the following two specific aims were developed to address these hypotheses.

1.7 Thesis Aims

Specific Aim 1: Establish that SGLT2 mediates the upregulation of AGT in PTC under high glucose conditions by increasing glucose reabsorption and ROS generation.

High glucose-induced AGT expression will be demonstrated in mPTC to confirm that the cells exhibit the characteristic response to glucose as previously reported^{113, 115}. Then, glycolytic activity in PTC will be measured during high glucose exposure, and the effects of pyruvate will be tested to demonstrate that glucose metabolism stimulates AGT expression. ROS generation will be measured in cells, and tempol will be used to show that ROS mediates the upregulation of AGT. Finally, the role of SGLT2-dependent glucose transport on AGT expression will be demonstrated by employing a gene silencing technique using SGLT2-specific shRNA.

Specific Aim 2: Demonstrate that AT1R activation enhances the upregulation of AGT expression and ROS generation under high glucose conditions in PTC.

Cells will be co-stimulated with high glucose and one of several Ang II concentrations within the physiological range of values found in the tubular fluid¹⁴⁷. Therefore, the results of these experiments will determine if Ang II enhances AGT augmentation by high glucose. In addition, PTC will be treated with an AT1R blocker at the beginning of high glucose treatment, which will demonstrate the contribution of AT1R activation by endogenous Ang II in AGT upregulation. Furthermore, SGLT2 expression will be quantified to determine if increased SGLT2 contributes to the upregulation of AGT by high glucose.

The findings in this study will help elucidate the molecular mechanisms governing AGT upregulation in the proximal tubule under diabetic conditions. Moreover, this study will delineate the events leading to intrarenal RAS activation in DM (Fig. 1.7.1).

FIGURE 1.7.1

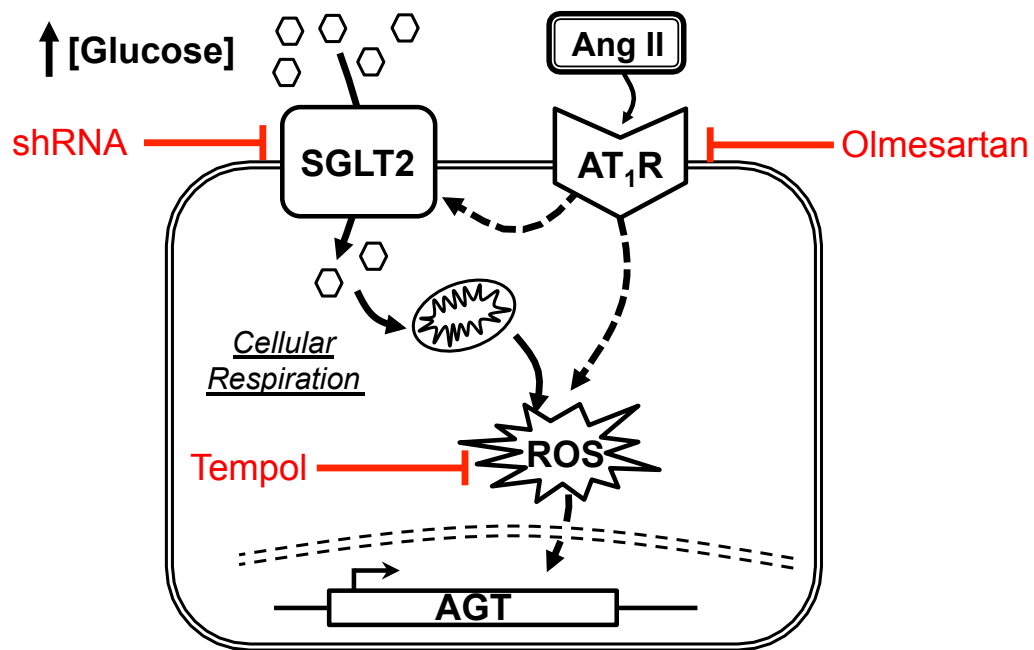


Figure 1.7.1: Proposed model of AGT upregulation by high glucose in proximal tubular cells. In this project, we will test the hypothesis that SGLT2-dependent glucose transport mediates the upregulation of AGT under high glucose conditions in PTC as a result of increased glucose metabolism and ROS generation. In addition, we will determine if AT₁R has an enhancing effect on glucose-induced AGT expression, possibly by augmenting SGLT2 expression.

CHAPTER 2 – MATERIALS AND METHODS

2.1 Cell Line

This cell line used in this project was provided by Dr. Ulrich Hopfer (Case Western Reserve University School of Medicine). The cells are an immortalized cell line derived from the Immortomouse™, a transgenic mouse which expresses the simian virus 40 large T antigen¹⁴⁸. Cells were isolated from the S1 segment of a male mouse proximal convoluted tubule cells (mPTC)^{149, 150}. After identifying the glomerulus, a 1- to 2-mm portion was dissected and grown on collagen-coated culture plate inserts and grown in medium with the following composition: 1:1 ratio (v/v) of Dulbecco Modified Eagle's Medium (DMEM) and Ham's F-12, aldosterone (10 nM), L-ascorbic acid 2-phosphate (50 µM), dexamethasone, (4 µg/ml), epidermal growth factor (10 ng/ml), insulin (5 µg/ml), sodium selenite (20 nM), transferrin (5 µg/ml), L-3,3',5-triiodothyronine (1 nM), HEPES (15 mM), sodium bicarbonate (1.2 mg/ml), penicillin G (100 U/ml) and streptomycin (100 µg/ml)¹⁵⁰.

In these experiments, mPTC culture was maintained in DMEM (Gibco), supplemented with 10% fetal bovine serum (FBS) (Gibco). Cells were incubated at 33 °C in a 5% CO₂ humidified environment (Fig. 2.1). Prior to high glucose treatment, cells were rinsed with PBS, and incubated in serum-free medium for 48 hours at 37 °C. Because sodium pyruvate is an energy source used by the

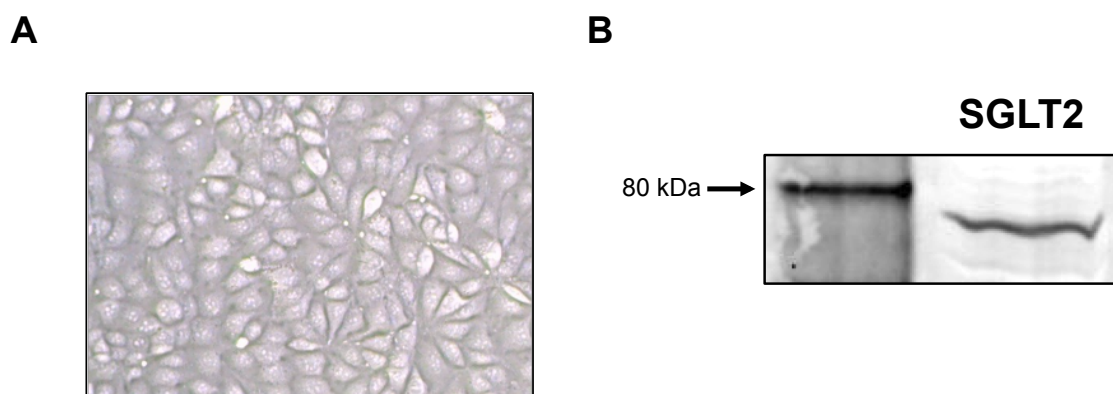
FIGURE 2.1

Figure 2.1: mPTC culture. (A) This PTC line was derived from the early proximal tubular segment, the primary site of SGLT2 expression and renal glucose reabsorption¹⁵⁰. (B) Immunoreactive band at ~73 kDa, the expected molecular weight of SGLT2⁶³.

mitochondria and would interfere with the experimental conditions, cells were serum-starved in pyruvate-free DMEM supplemented with 5 mM glucose.

2.2 Drugs

mPTC were treated with olmesartan, an AT1R blocker, to test the effects of endogenous Ang II. 1 mM olmesartan was added to the cells at the beginning of high glucose treatment. Olmesartan has been shown to block AT1R activation at the micromolar range in cultured PTC, thus this concentration should be sufficient ¹⁵¹. Tempol (Sigma) is an antioxidant that neutralizes ROS by catalyzing the disproportionation of superoxide and was used to neutralize ROS generation. Tempol was added to cells 1 hour before high glucose treatment. Tempol has cytotoxic effects at high concentrations ¹⁵², but 2.5 mM did not affect the viability of the cells.

2.3 High Glucose Treatment

mPTC were exposed to glucose levels chosen for their clinical and physiological relevance. During treatment, cells were treated with serum-free DMEM supplemented with D-glucose to a final concentration of 5 mM, 10 mM, 15 mM, or 25 mM. 5 mM, representing a normal plasma glucose level, was used as control conditions. 10 mM, 15 mM and 25 mM represent hyperglycemic conditions found in untreated diabetes mellitus ¹⁵³. The medium during treatment and serum-starvation was free of pyruvate, bicarbonate, and HEPES buffer, which would interfere with the experimental results.

2.4 Quantitative Real-Time RT-PCR

Reverse transcriptase polymerase chain reaction (RT-PCR) is a method for detecting mRNA transcripts by first creating a cDNA strand and amplifying it using PCR. Quantitative real-time RT-PCR (qPCR) allows for the relative expression levels of target genes to be determined by detecting the amount of amplification product at each PCR cycle and comparing it to a standard curve using known quantities of target mRNA. Increased levels of mRNA template in a reaction will cause faster rate of amplification¹⁵⁴ (Fig. 2.4).

The Taqman system utilizes an oligonucleotide with a covalently linked fluorescent marker on the 5'-end and a quencher molecule located on the 3' end, which prevents fluorescence when the molecules are in close proximity. During the extension phase of the PCR reaction, the probe is degraded by the 5' → 3' exonuclease activity of Taq polymerase, which releases the fluorescent marker causing it to fluoresce^{155, 156}. Therefore, the level of fluorescence is proportional to the number of amplification products. Detecting fluorescence levels during each cycle allows for the rate of amplification to be quantified¹⁵⁶.

Experimental Protocol for qPCR

After high glucose treatment, cells were rinsed with PBS and mRNA was isolated using an RNeasy Mini Kit (QIAGEN). 100 ng RNA were combined with Brilliant II QRT-PCR 1-Step Master Mix (Agilent), and amplified using a Mx3005P

FIGURE 2.4

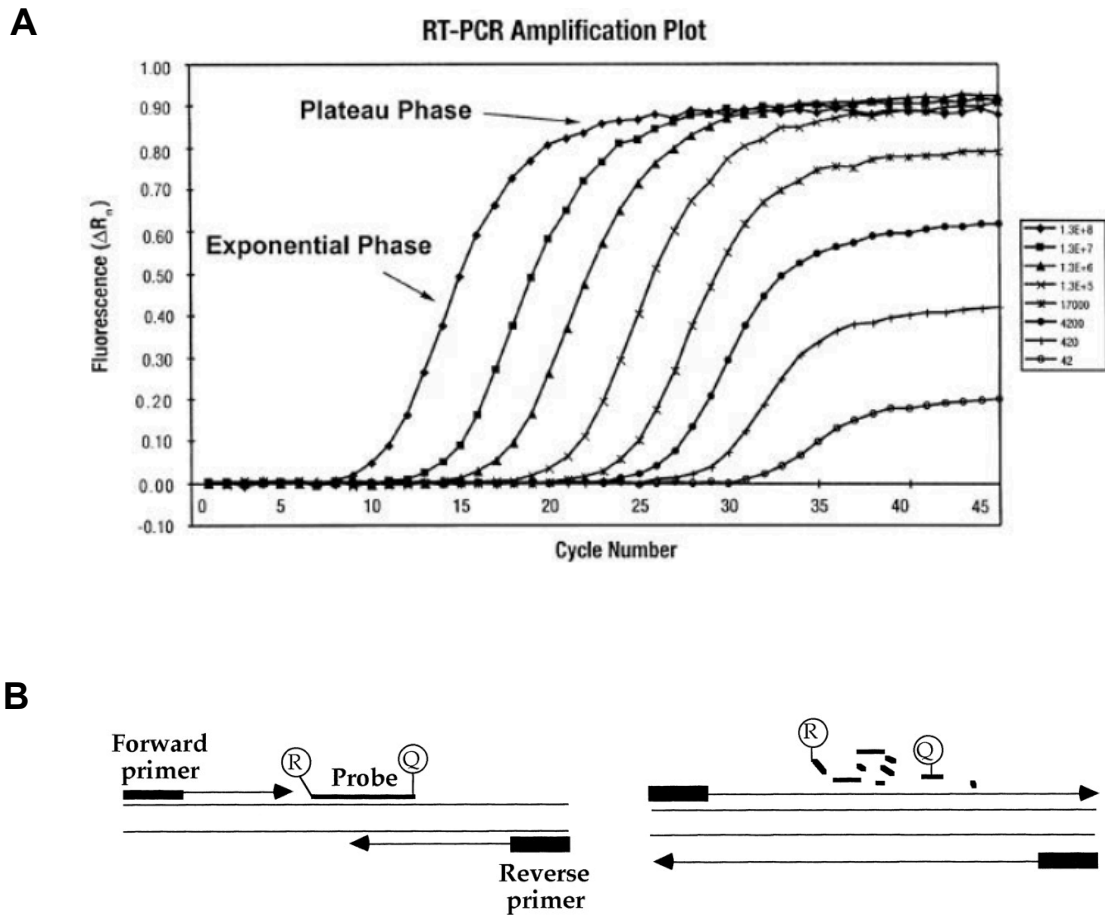


Figure 2.4: Overview of qPCR. (A) Relative expression levels can be assessed by when the cycle reaches the exponential phase of amplification. Adapted from Freeman et al., 1999¹⁵⁴. (B) Taqman probes are designed with a fluorescent marker covalently attached to the 5'-end and a quencher molecule on the 3'-end. The exonuclease activity cleaves the probe, decoupling it from the quencher molecule. Adapted from Gelmini et al., 1997¹⁵⁶.

system (Stratagene). C_T analysis was performed using MxPro Software (Agilent). Samples were analyzed in triplicate and GAPDH was used as an internal control.

2.5 Western Blot Analysis

Total cell lysates were prepared in lysis buffer (50 mM Tris-HCl (pH 8.0), 0.1% SDS, 0.5% sodium deoxycholate, 1% NP-40, 150 mM NaCl) containing 0.3% Protease Inhibitor Cocktail (Sigma), and 1 mM EDTA. Lysates were combined with Sample Buffer (4X) (Life Technologies) and NuPAGE Sample Reducing Agent (10X) (Life Technologies). Gel electrophoresis was performed using approximately 40 µg of protein per lane in a NuPAGE 4-12% Bis-Tris Gel (Life Technologies) and transferred to a 0.22 µm pore size nitrocellulose membrane. After transfer, membranes were blocked in Odyssey Blocking Buffer (LI-COR). All washes were performed in PBS-T. Primary antibodies included angiotensinogen (IBL; Cat. 28101), GAPDH (Santa Cruz Biotechnology; Cat. Sc-32233), and SGLT2 (Abcam; Cat. ab37296). Secondary antibodies were Anti-Rabbit or Anti-Mouse IgG (LI-COR). All antibody dilutions were performed in Odyssey Blocking Buffer. Membranes were detected using an Odyssey Infrared Imaging System (LI-COR).

2.6 ROS Detection

ROS generation was detected using 2',7'-dichlorodihydrofluorescein diacetate (H₂DCF-DA) (Life Technologies), which is a chemically reduced form of the compound fluorescein. After entering the cell, H₂DCF-DA is deacetylated by

intracellular esterases and subsequently oxidized by H_2O_2 and other ROS to create the fluorescent molecule DCF¹⁵⁷ (Fig. 2.6). Because $\text{H}_2\text{DCF-DA}$ is oxidized by several types of ROS, it is useful as an indicator of overall oxidative stress, and not any specific ROS molecule¹⁵⁸.

Experimental Protocol for ROS Detection

ROS was detected using a modified version of a protocol previously reported to measure ROS in renal PTC¹⁵⁹. Briefly, a 10 mM working stock of $\text{H}_2\text{DCF-DA}$ was prepared in DMSO and made fresh for each use. After 11 hours treatment in normal or high glucose, cells were treated with 20 μM $\text{H}_2\text{DCF-DA}$ or DMSO (vehicle control) at 37 °C for 1 hour. Using this process, ROS was also detected in samples after serum-starving to determine baseline ROS levels at the beginning of treatment. After incubation, cell culture medium was aspirated and cells were rinsed 3 times in PBS to remove any residual probe.

Fluorescence was detected using a FLUOstar OPTIMA microplate reader (BMG Labtech) using a 492 nm excitation filter and 520 nm emission filter. Live-cell images were captured using an EVOS FI microscope (AMG). Baseline ROS levels were subtracted from the treated samples, so the data reflect the change in fluorescence between normal and high glucose treatment.

2.7 Metabolic Activity Analysis

Glycolytic activity was measured using an XF Extracellular Flux Analyzer (Seahorse Bioscience), which detects the extracellular acidification rate (ECAR)

FIGURE 2.6

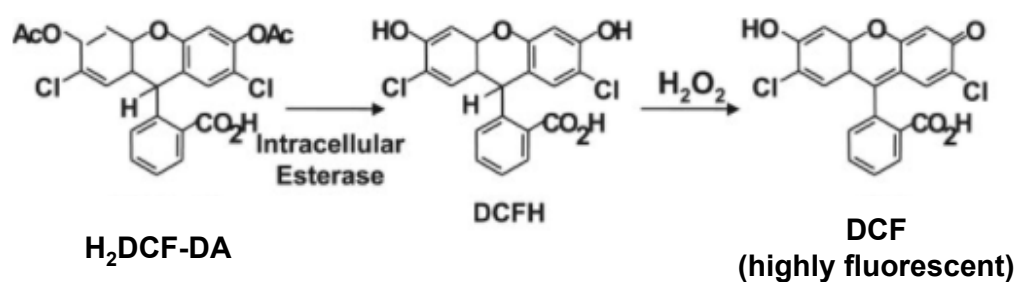


Figure 2.6: ROS detection using $\text{H}_2\text{DCF-DA}$. $\text{H}_2\text{DCF-DA}$ enters the cell where it is deacetylated by intracellular esterases and oxidized when exposed to H_2O_2 and other ROS. Because it is oxidized by several ROS molecules, it is an indicator of general oxidative stress within the cell ¹⁵⁸.

and oxygen consumption rate (OCR) of cells. After glycolysis, pyruvate is converted to lactate and a hydrogen atom or oxidized in the mitochondria, which consumes oxygen. Therefore, the rate of change in H^+ and O_2 concentrations represents the glycolytic activity and mitochondrial respiration of the cells, respectively^{160, 161}. The extracellular flux analyzer performs real-time measurements of these parameters to determine the metabolic profile of the cells (Fig. 2.7).

Experimental Protocol to Measure Glycolytic Activity

To measure ECAR in mPTC, cells were seeded on cell culture plates (Seahorse Bioscience) at a density of 4.0×10^5 cells per well and incubated at 33 °C for 24 hours. Wells were rinsed in PBS and 500 μ L serum-free DMEM was added to each well, and the plate was moved to 37 °C. After serum-starvation, the plate was incubated at 37 °C in a CO_2 -free incubator for 1 hour before treatment to remove residual CO_2 trapped in the plastic, which can cause acidification and alter results.

The plate was then attached to a pre-calibrated Seahorse XF cartridge and loaded into the XF^e24 extracellular flux analyzer. Extracellular acidification was measured every 10 minutes. After 3 measurement cycles, cells were injected with 75 μ L DMEM containing glucose to a final concentration of 5 mM, 10 mM, 15 mM, or 25 mM glucose in each well (N = 5). Measurements were taken every 10 minutes for 150 minutes.

FIGURE 2.7

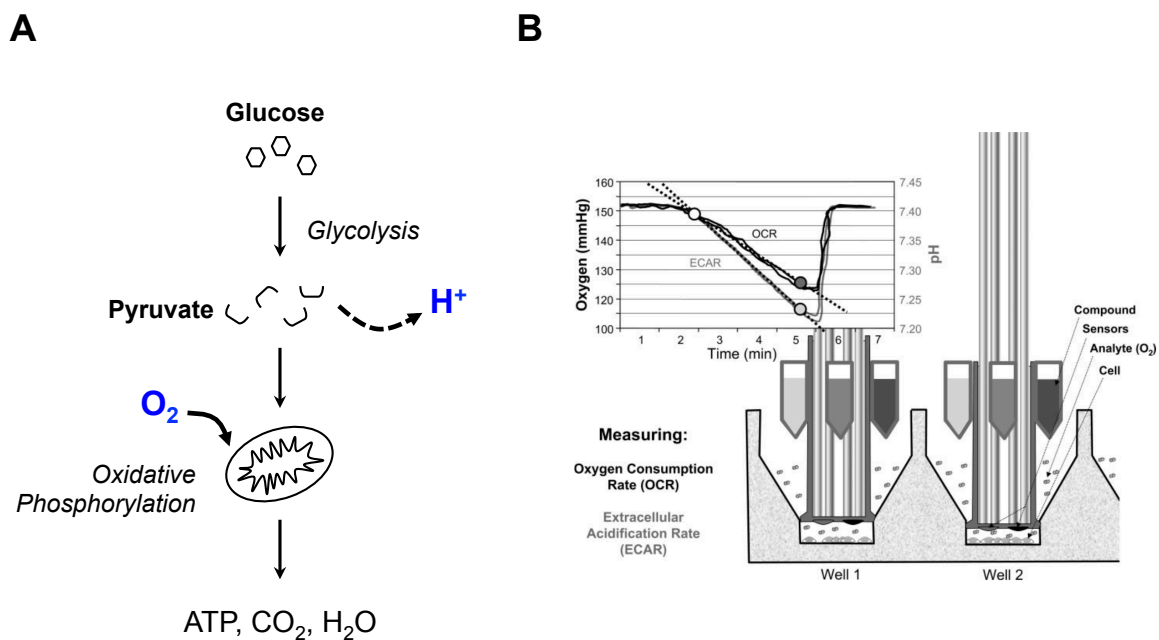


Figure 2.7: Metabolic analysis using extracellular flux. (A) After glycolysis, protons are generated as a by-product, which increases the rate of extracellular acidification. During mitochondrial respiration, oxygen acts as an electron acceptor and is converted into H_2O , causing a decrease in O_2 concentration. (B) Diagram of the function and measurement of the Seahorse XF analyzer¹⁶¹. Measurements are taken directly above the cells to measure the changes in acidification and oxygen consumption.

2.8 SGLT2 Gene Expression Knockdown

SGLT2 knockdown was performed in mPTC using short hairpin RNA (shRNA). shRNA is a technique used to knockdown gene expression by targeting specific RNA sequences for degradation. An effective technique to achieve shRNA-mediated gene knockdown in eukaryotic cells is to insert the shRNA sequence into plasmid DNA¹⁶². After transfection, the shRNA sequence is expressed and processed by the enzyme Dicer to generate siRNAs which then bind to a complementary RNA sequence on the target mRNA in a process guided by the RNA-induced silencing complex (RISC). The target mRNA is then degraded, thus preventing the translation of the target gene¹⁶³.

Experimental Protocol for shRNA-Mediated Gene Knockdown

SGLT2 expression was knocked down using an shRNA plasmid (Creative Biogene) targeting base 628 of the mouse Slc5a2 gene (Fig. 2.8) using the following sequence: 5'-GCCTTCATCCTCACTGGTTAT-3'. *Escherichia coli* cells containing the plasmid were grown in LB broth supplemented with kanamycin (50 µg/mL). The plasmid DNA was harvested using a QIAprep Spin Miniprep Kit (QIAGEN) and eluted in ddH₂O to a final concentration of 1.1 µg/mL.

After transfection with anti-SGLT2 or negative control plasmid, cells were serum-starved for 48 hours at 37 °C. Cells were then treated with 5 mM or 15 mM glucose for 12 hours.

FIGURE 2.8

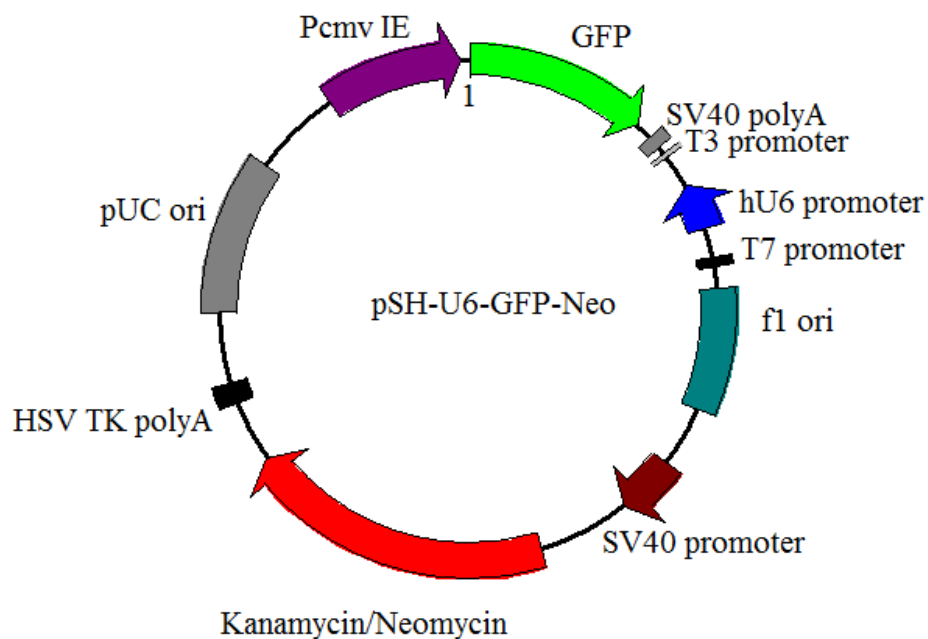


Figure 2.8: Vector map of the plasmid containing the shRNA sequence targeting SGLT2. (Creative Biogene). The vector contained the sequence targeting mouse SGLT2, designed to silence SGLT2 expression, or a negative control sequence. The kanamycin resistance gene allowed for plasmid amplification in *E. coli* cells.

2.9 Electroporation

The shRNA plasmid was transfected into the cells using electroporation. Because plasmid DNA is a large, negatively charged molecule, it is very difficult to transfer across the lipid bilayer of eukaryotic cells. Electroporation utilizes an electric field applied to the cells to increase the permeability of the plasma membrane^{164, 165}. This process creates aqueous pores in the membrane which facilitate the entry of plasmid DNA into the cell, permitting the transfection of the shRNA¹⁶⁴.

Experimental Protocol for Electroporation

mPTC were transfected using a Neon Transfection System (Invitrogen). After trypsinization, mPTC were washed in PBS and resuspended in Neon Suspension Buffer R with 1 µg plasmid DNA per sample (shRNA plasmid or negative control plasmid). Using the protocol from the manufacturer, electroporation conditions were optimized to maximize transfection efficiency while minimizing cell death. The conditions used in the experiment were as follows: 1100 V, 40 ms, 1 pulse per sample. Cells were plated on 24-well plates at a density of 100,000 cells per well in DMEM supplemented with 10% FBS and incubated at 33 °C for 12 hours. Transfection efficiency was determined by the percentage of GFP-expressing cells under a fluorescent microscope. When the cells were expressing GFP, they were rinsed with PBS and serum-starved at 37 °C for 48 hours before glucose treatment.

2.10 Statistical Analysis

For the experiments in Specific Aim 1, statistical analysis was performed using Student's t-test or one-way repeated measures analysis of variance (ANOVA). Data obtained in Specific Aims 2 was analyzed using two-way repeated measures ANOVA, with glucose concentration and Ang II treatment as the two factors. The Bonferroni correction was applied for multiple comparisons testing. Statistical significance is defined as $P < 0.05$. Data are presented as means \pm standard error.

CHAPTER 3 – SPECIFIC AIM 1

Establish that SGLT2 mediates the upregulation of AGT in PTC under high glucose conditions by increasing glucose reabsorption and ROS generation.

3.1 Research Design for Specific Aim 1

As described above in Chapter 1, Specific Aim 1 is designed to test the hypothesis that SGLT2 mediates the upregulation of AGT expression in PTC under high glucose conditions. Therefore, experiments were performed to address the following sub-aims:

- 1) Confirm that high glucose treatment stimulates AGT expression levels in mPTC.
- 2) Demonstrate that exposure to high glucose increases glucose metabolism in PTC, and that glucose metabolites stimulate AGT expression.
- 3) Demonstrate that ROS accumulation is increased in mPTC under high glucose conditions, and AGT upregulation by high glucose is ROS-dependent.
- 4) Establish that SGLT2-dependent glucose transport is required for high glucose-induced AGT expression using shRNA-mediated gene knockdown of SGLT2.

3.2 Results

3.2.1 AGT expression levels are increased by exposure to high glucose conditions.

To establish this mPTC line as an experimental model of glucose-stimulated AGT upregulation, AGT expression levels were measured after high glucose exposure to characterize the cellular response (Fig. 3.1). AGT protein levels were increased in 25 mM glucose compared to 5 mM starting after 6 hours treatment (2.40 ± 0.05 -fold). The maximum AGT induction by high glucose was observed after 12 hours treatment (7.92 ± 0.06 -fold). While AGT protein levels were comparatively low in cells treated with 5 mM glucose, there was a downward trend over the treatment time between 3 and 24 hours, but it was not significant. Additionally, AGT in 25 mM glucose increased up to 12 hours compared to 5 mM, but sharply decreased by 75% between 12 and 24 hours. At 24 hours, AGT was still higher than control (6.25 ± 0.10 -fold), but the absolute levels were significantly lower than 6 and 12 hours. GAPDH levels remained fairly constant during high glucose treatment. After 24 hours treatment, AGT mRNA levels were very low in 5 mM glucose. In 25 mM glucose, AGT was upregulated (31.1 ± 3.5 -fold) compared to 5 mM.

After 12 hours treatment in 5 mM, 15 mM, or 25 mM glucose, AGT protein levels were barely detectable in 5 mM. AGT protein was increased in 15 mM (4.4 ± 0.2 -fold) and 25 mM (4.6 ± 0.2 -fold) glucose compared to control. There was no difference in AGT augmentation between 15 mM and 25 mM. In addition, AGT

FIGURE 3.1

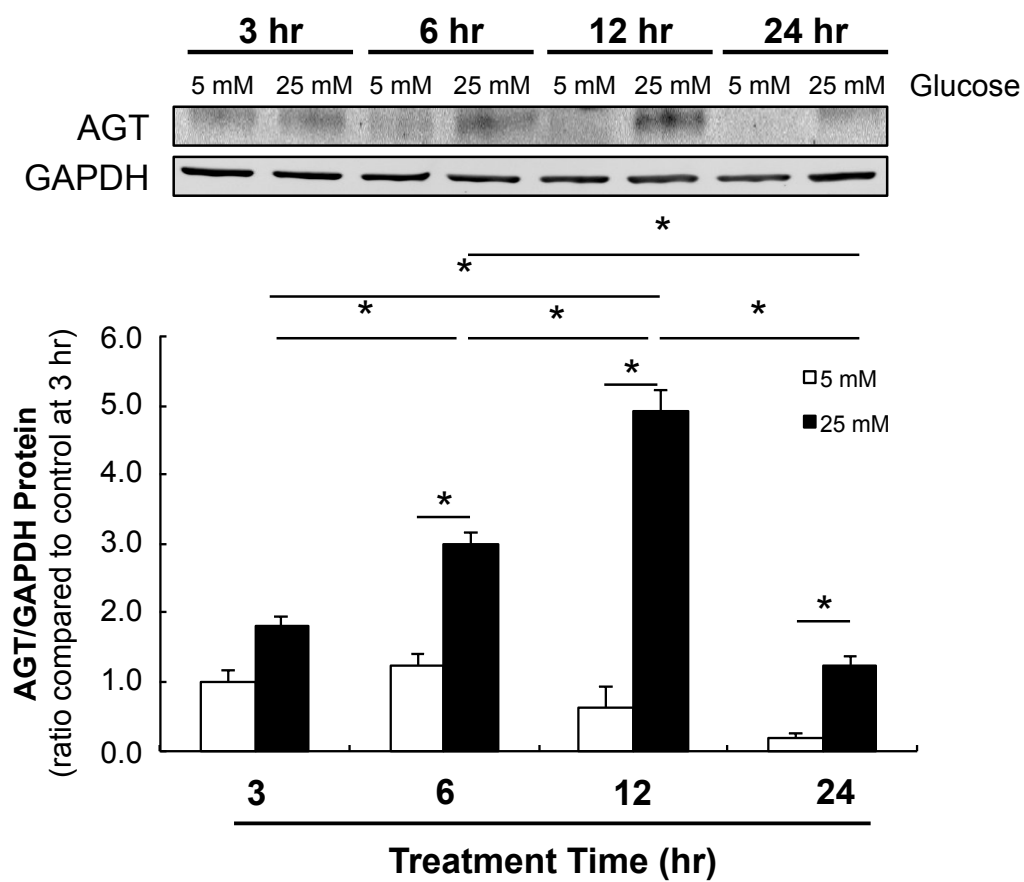
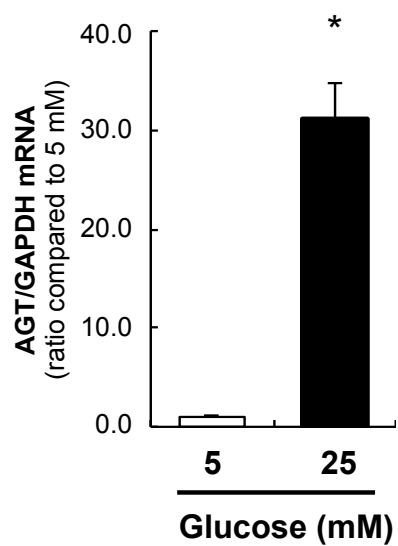
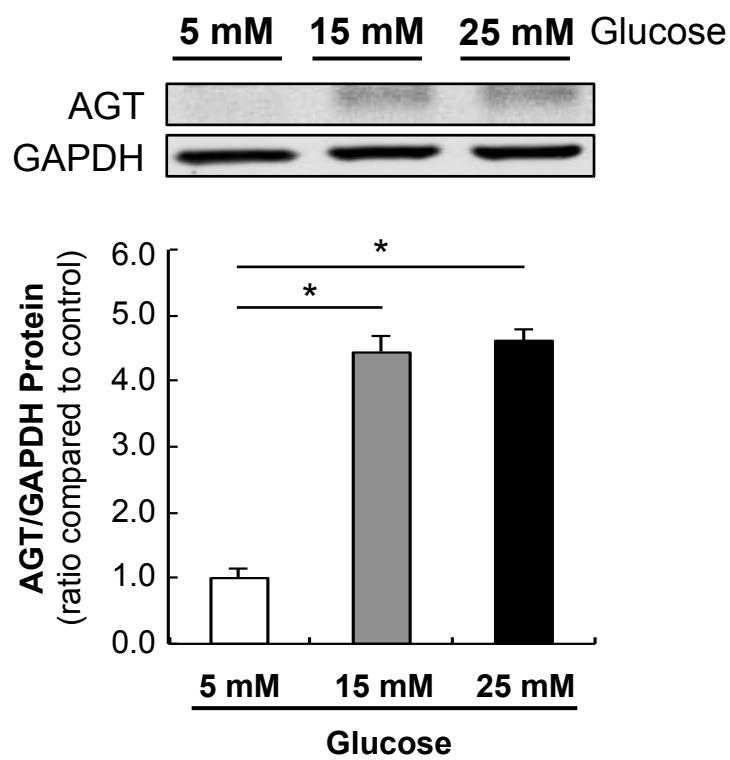
A**B**

FIGURE 3.1

C



D

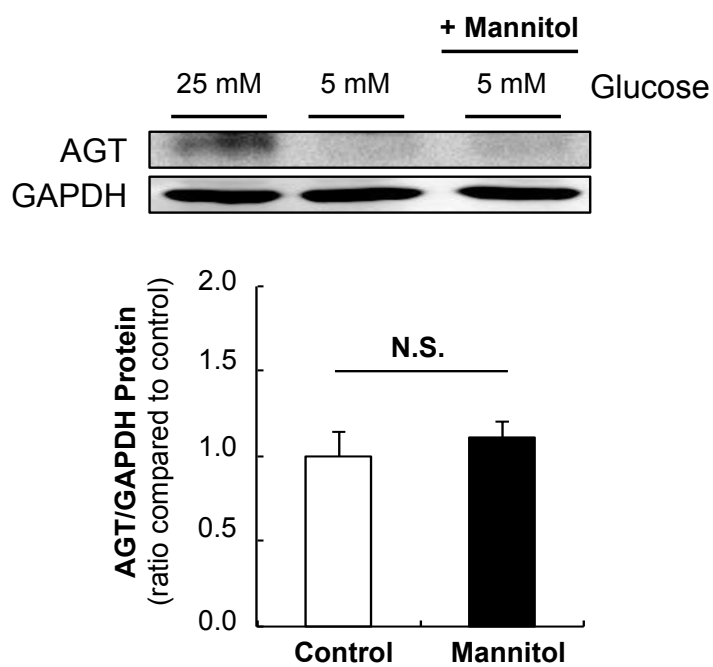


Figure 3.1: High glucose exposure stimulates AGT expression in mPTC. (A)

AGT protein levels at 3, 6, 12, or 24 hours treatment with 5 mM or 25 mM glucose. (B) AGT mRNA levels were increased after 24 hours treatment in 5 mM or 25 mM glucose. (C) AGT protein levels at 12 hours treatment in 5 mM, 15 mM, and 25 mM glucose. (D) AGT protein levels at 12 hours treatment in 5 mM glucose with or without 20 mM mannitol. 25 mM glucose was used as a positive control. The data represent the mean \pm SE (N = 3, or 4). Asterisk indicates significant difference ($P < 0.05$).

expression was not augmented after exposure to mannitol (osmotic control). The positive control sample showed clear augmentation (Fig. 3.1).

3.2.2 AGT is augmented by increased glucose metabolism

The effects of high glucose exposure on glucose metabolism in PTC were quantified (Fig. 3.2). Baseline ECAR levels were variable, but not different between groups. In 5 mM treated cells, ECAR steadily declined over the course of treatment, before leveling off at approximately 2.0 mpH/min. Starting 30 minutes after the addition of glucose, ECAR increased in 15 mM or 25 mM glucose compared to control by 1.88 ± 0.10 fold and 1.97 ± 0.23 fold, respectively, indicating enhanced glycolytic activity. The maximum increase in ECAR compared to 5 mM was observed 40 minutes after the addition of glucose (3.10 ± 0.28 -fold, 2.74 ± 0.20 -fold, and 2.75 ± 0.34 -fold, respectively). After 40 minutes, ECAR began to decline, and was not statistically different from 5 mM at 80 minutes. At each time point, ECAR was similar between the different high glucose concentrations.

Pyruvate is a metabolite of glucose produced after glycolysis. AGT expression in response to sodium pyruvate was tested to demonstrate that AGT upregulation is stimulated by glucose metabolites. After 24 hours, AGT mRNA levels were enhanced in cells treated in 5 mM glucose supplemented with 1 mM pyruvate 10.74 ± 1.03 -fold compared to control (Fig. 3.3), supporting the model of AGT upregulation occurring as a consequence of increased glucose metabolism.

FIGURE 3.2

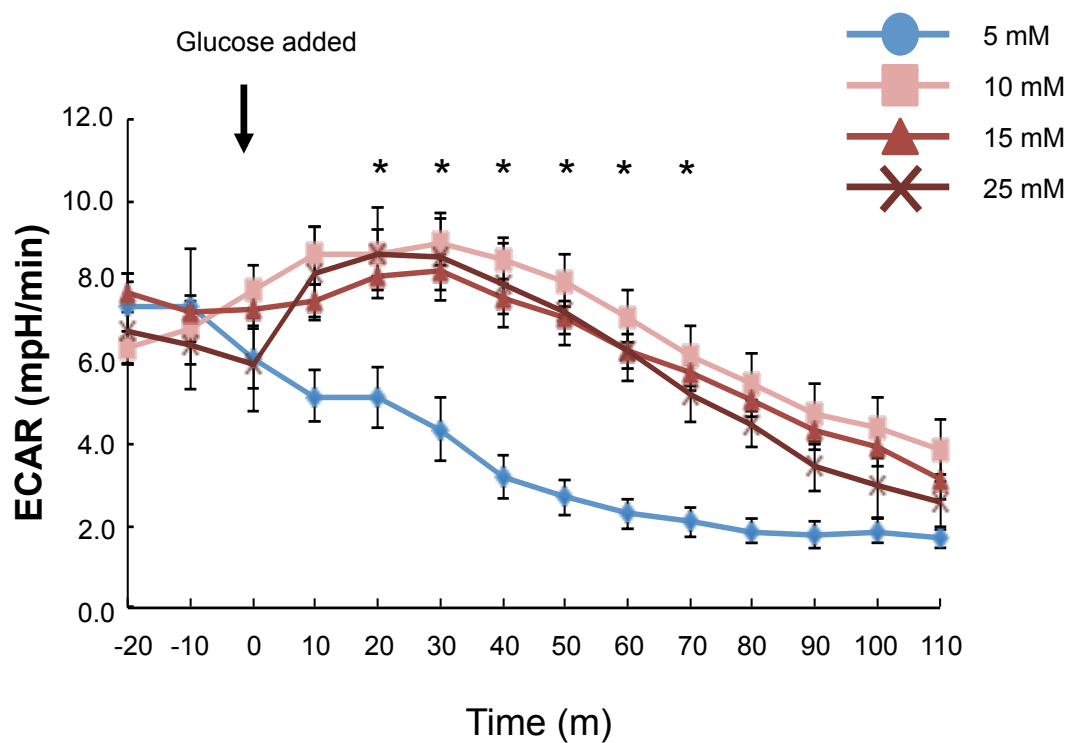


Figure 3.2: High glucose exposure induces glycolytic activity in PTC.

Extracellular acidification rate in mPTC treated with 5 mM, 10 mM, 15 mM, or 25 mM glucose. The data represent means \pm SE (N = 5). Asterisk indicates ($P < 0.05$) vs. control.

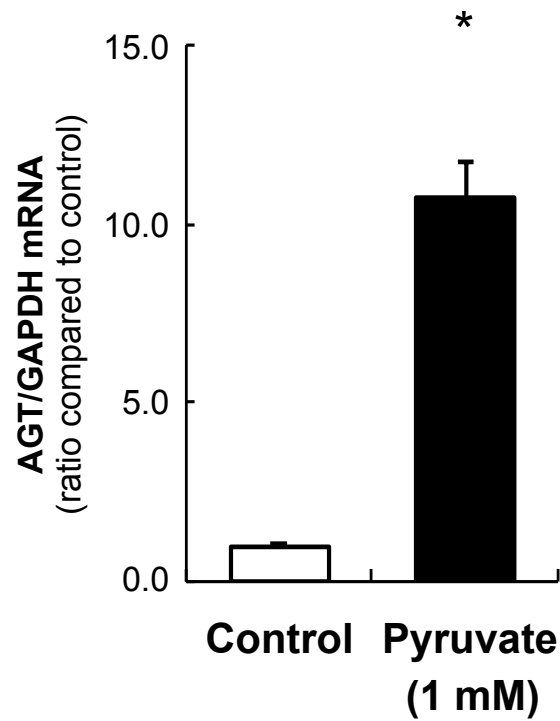
FIGURE 3.3

Figure 3.3: AGT expression is stimulated by pyruvate. AGT mRNA levels after 24 hours treatment with sodium pyruvate (1 mM). Treatment with pyruvate enhanced AGT mRNA levels, suggesting that glucose metabolism stimulates AGT expression. The data represent means \pm SE (N = 4). Asterisk indicates ($P < 0.05$) vs. control.

3.2.3 Increased ROS generation mediates glucose-induced AGT expression in mPTC.

ROS accumulation over the 12-hour treatment period was determined by quantifying ROS-induced fluorescence after treatment compared to baseline levels (Fig. 3.4). Fluorescence was low, but observable in 5 mM treated cells. However, in cells treated with 25 mM glucose, fluorescence levels were noticeably brighter. The non-probe treated samples showed no background fluorescence. ROS levels were quantified using a microplate reader. After subtracting background ROS (at 0 hours), cells treated with 25 mM glucose exhibited higher fluorescence levels (3.03 ± 0.29 -fold) compared to 5 mM glucose, demonstrating that high glucose exposure promotes ROS generation in mPTC.

To determine the effects of ROS generation on glucose-induced AGT expression, cells were pretreated with the antioxidant tempol, which neutralizes ROS (Fig. 3.5). After 12 hours treatment, in the absence of tempol, AGT was upregulated in high glucose treated cells (311.9 ± 29.0 -fold) compared to control. In tempol-treated cells, AGT augmentation by high glucose was decreased by 77% compared to untreated cells (71.2 ± 3.16 -fold compared to normal glucose). AGT was barely detectable in cells in 5 mM glucose, and tempol had no effect on AGT expression. In addition, GAPDH levels were not affected by tempol treatment.

FIGURE 3.4

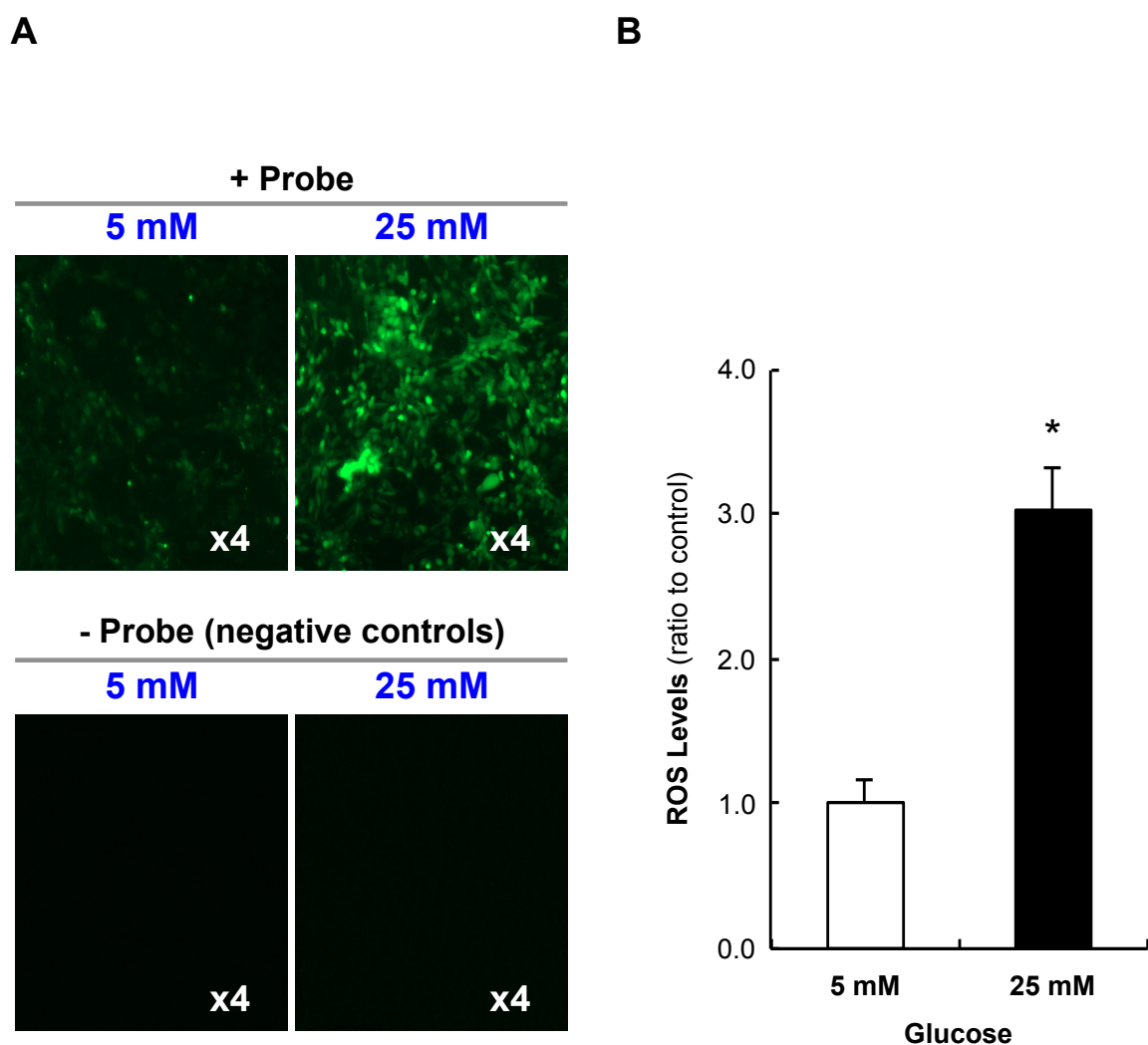


Figure 3.4: High Glucose Treatment Promotes ROS Accumulation. (A) Representative image of ROS-induced fluorescence in cells treated with 5 mM or 25 mM glucose after 12 hours. (B) Quantification of fluorescence in the samples. The data represent means \pm SE (N = 5). Asterisk indicates ($P < 0.05$) vs. control.

FIGURE 3.5

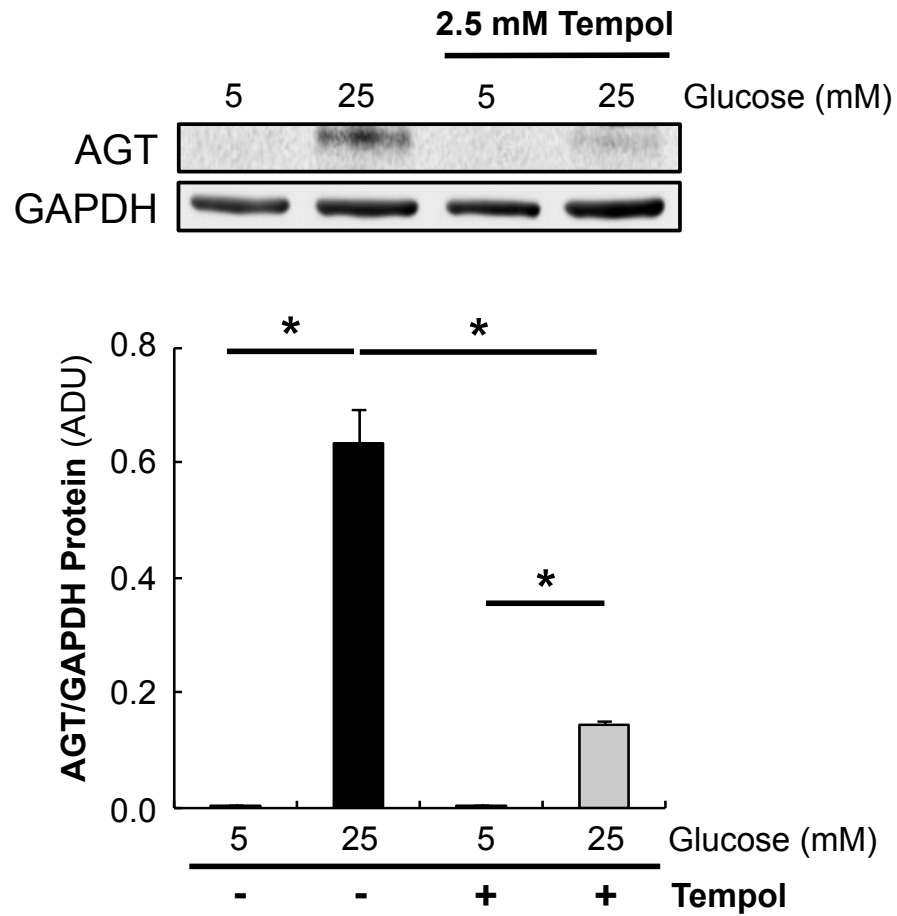


Figure 3.5: ROS generation is required for AGT augmentation under high glucose conditions. AGT protein levels after 12 hours treatment in 5 mM or 25 mM glucose with or without the addition of 2.5 mM tempol. The data represent means \pm SE (N = 4). Asterisk indicates ($P < 0.05$) vs. control.

3.2.4 SGLT2 mediates glucose-induced AGT upregulation.

To establish the role of SGLT2 in AGT augmentation, the effects of high glucose treatment on AGT expression were measured during SGLT2 knockdown. mPTC were transfected with plasmid DNA expressing an shRNA sequence targeting SGLT2 or a negative control sequence (Fig. 3.6). 12 hours after electroporation, approximately 60% of cells expressed GFP. The percentage of GFP-expressing cells was not different between the negative control plasmid and the SGLT2 shRNA plasmid.

After serum-starvation, cells were treated in 5 mM or 15 mM glucose for 12 hours (Fig. 3.6). Overall, AGT bands were weaker than in previous experiments, and AGT expression was variable in 15 mM glucose. In cells receiving the negative control plasmid, AGT protein levels were stimulated by 15 mM glucose (2.2 ± 0.5 -fold) compared to 5 mM. However, in cells transfected with the shRNA, AGT expression was not different between 5 mM and 15 mM glucose treatment. While it appears that AGT was lower in 15 mM compared to 5 mM, it was not significant. In 5 mM-treated cells, shRNA had no effect on AGT expression compared to the control plasmid. This indicates that SGLT2 knockdown prevented the enhancing effects of high glucose. GAPDH expression was slightly lower in the shRNA plasmid compared to the control plasmid.

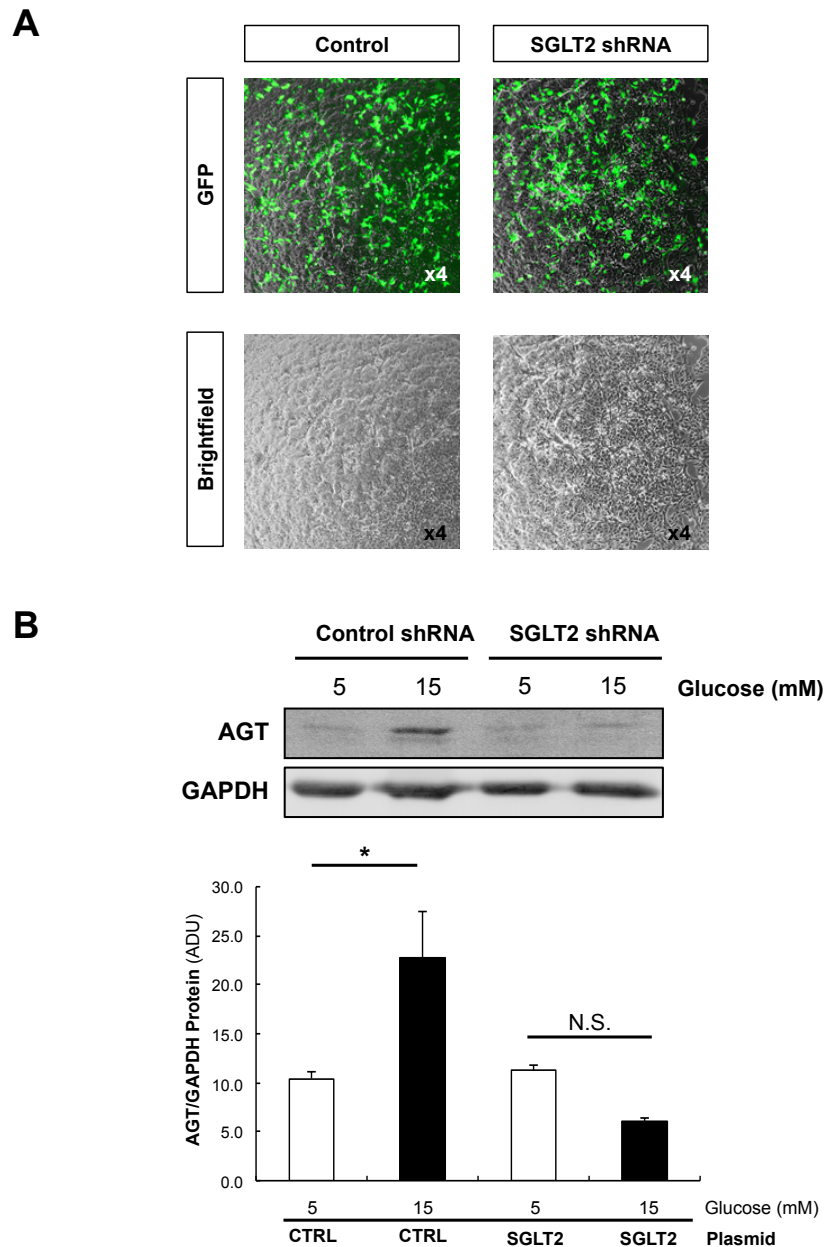
FIGURE 3.6

Figure 3.6: SGLT2 mediates glucose-induced AGT augmentation. (A) GFP expression 12 hours after electroporation. GFP labeling indicates successful transfection. (B) AGT protein levels in 5 mM or 15 mM glucose at 12 hours in cells transfected with control plasmid or shRNA against mouse SGLT2. The data represent means \pm SE (N = 3). Asterisk indicates ($P < 0.05$) vs. control.

CHAPTER 4 – SPECIFIC AIM 2

Demonstrate that AT1R activation enhances the upregulation of AGT expression and ROS generation under high glucose conditions in PTC.

4.1 Research Design for Specific Aim 2

As described in Chapter 1, Specific Aim 2 was designed to test the hypothesis that SGLT2-dependent glucose transport and glucose-induced AGT augmentation are enhanced by Ang II and AT1R activation. Experiments were performed to address the following sub-aims:

- 1) Determine if Ang II enhances glucose augmentation by high glucose.
- 2) Determine if SGLT2 expression is enhanced by treatment with high glucose and/or Ang II.

4.2 Results

4.2.1 AT1R activation does not enhance high glucose-induced AGT upregulation.

To determine if endogenous AT1R activation contributes to AGT augmentation by high glucose, mPTC were pretreated for 60 minutes with 1 mM olmesartan, an AT1R blocker (Fig. 4.1). AGT augmentation induced by high

FIGURE 4.1

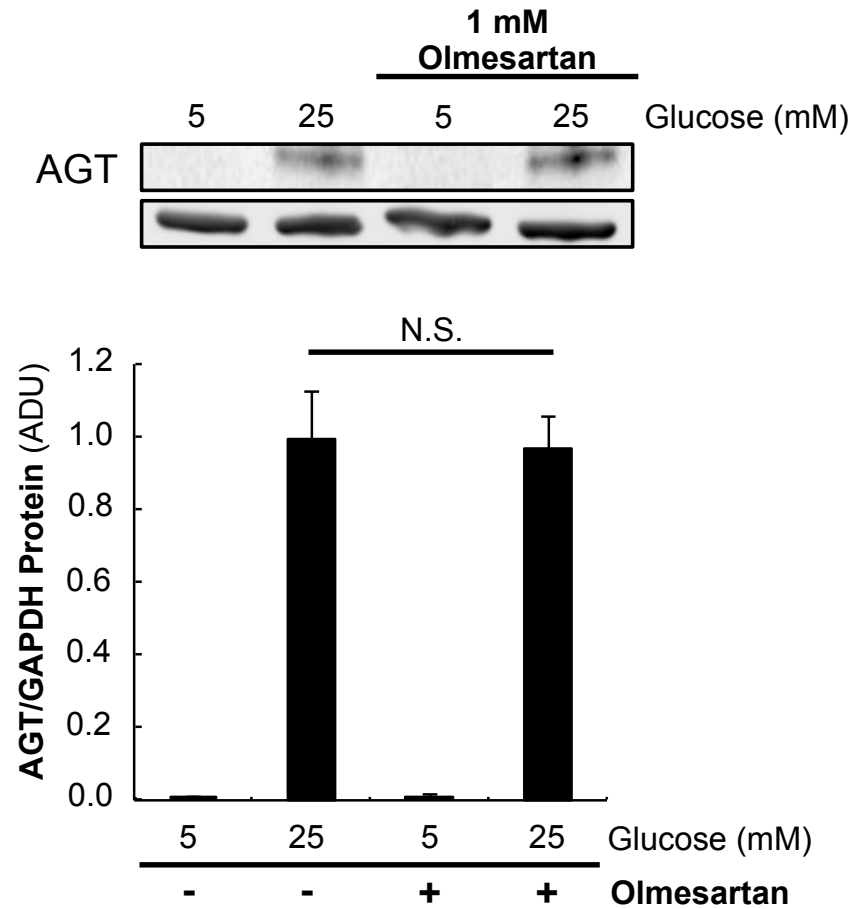


Figure 4.1: AT1R activation is not required for AGT upregulation by high glucose. AGT protein levels after 12 hours treatment in 5 mM or 25 mM glucose, with or without 1 mM olmesartan. The data represent means \pm SE (N = 4). Asterisk indicates ($P < 0.05$) vs. control.

glucose was not different between cells without olmesartan treatment (128.3 ± 16.8 -fold) and with olmesartan treatment (124.9 ± 11.7 -fold). Thus, AGT upregulation was not attenuated by olmesartan. Olmesartan did not affect AGT levels under normal glucose conditions.

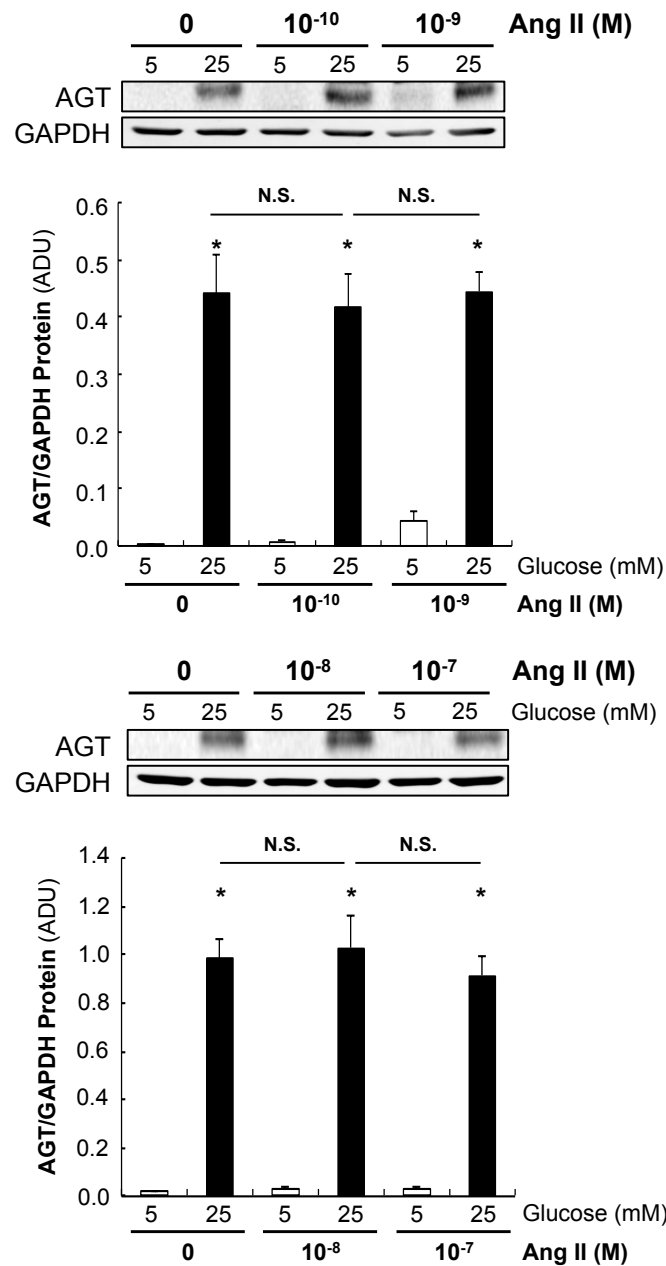
To test the effects of Ang II on high glucose-induced AGT expression, mPTC were co-stimulated with 25 mM glucose and varying doses of Ang II within the physiological range in the tubular fluid ³². Cells were treated with relatively low-doses (0 M, 10^{-10} M, or 10^{-9} M) and high doses (0 M, 10^{-8} M, or 10^{-7} M) for 12 hours (Fig. 4.2).

At all Ang II doses, AGT protein levels were low in normal glucose conditions. AGT was upregulated by high glucose compared to control (5 mM, 0 M Ang II). At 5 mM glucose, there is an upward trend in AGT expression by 10^{-9} M Ang II, but it was not significant. However, AGT induction during co-stimulation with high glucose and Ang II was not different than high glucose alone.

4.2.2 SGLT2 expression is not enhanced by high glucose or Ang II

To test if AT1R activation stimulates SGLT2 expression in PTC, cells were co-stimulated with glucose and Ang II as described above, and SGLT2 protein levels were evaluated after 12 hours (Fig. 4.3). Similarly, in normal glucose conditions, SGLT2 levels trend higher in 10^{-10} M and 10^{-9} M Ang II, but it was also not significant. Higher doses of Ang II did not show any clear trends. In high glucose conditions, Ang II did not enhance SGLT2. The data from these experiments show that high glucose and Ang II had no effect on SGLT2

expression. In cells without Ang II treatment, there is an upward trend in SGLT2 protein in high glucose compared to normal glucose treatment, but it was not statistically significant.

FIGURE 4.2**Figure 4.2: Ang II does not enhance glucose-induced AGT augmentation.**

AGT protein levels in cells treated with 5 mM or 25 mM glucose, and Ang II: 0, 10^{-10} M, or 10^{-9} M (top); 0, 10^{-8} M, or 10^{-7} M (bottom). The data represent means \pm SE (N = 4). Asterisk indicates ($P < 0.05$) vs. control.

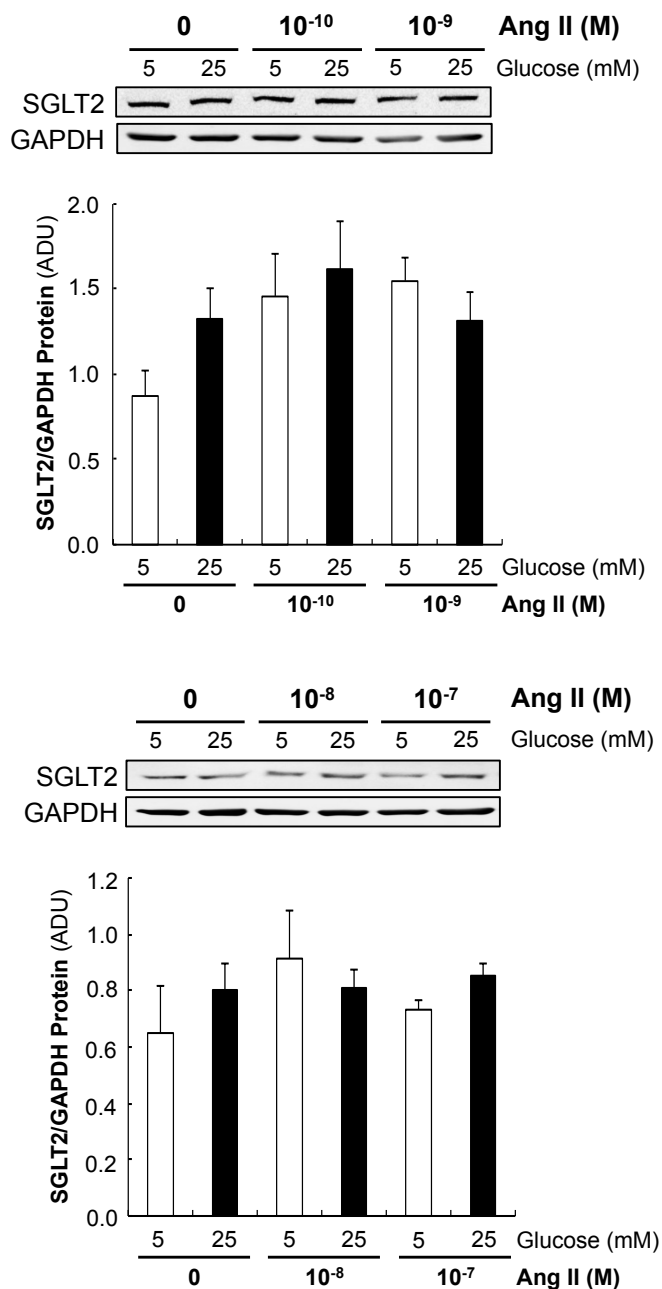
FIGURE 4.3

Figure 4.3: SGLT2 protein levels are not enhanced by high glucose or Ang II. SGLT2 protein levels in cells treated with 5 mM or 25 mM glucose, and Ang II: 0, 10^{-10} M, or 10^{-9} M (top); 0, 10^{-8} M, or 10^{-7} M (bottom). The data represent means \pm SE (N = 4). Asterisk indicates ($P < 0.05$) vs. control.

CHAPTER 5 – DISCUSSION AND CONCLUSIONS

Proximal Tubule Cell Line

This study demonstrates that AGT expression in mPTC is upregulated under hyperglycemic conditions (Fig. 3.1), which has been previously shown in animal models of diabetes ¹¹⁴ and in cultured PTC ¹¹⁶. In the mPTC line used in this research, virtually all of the cells exhibited a uniform, cuboidal “cobblestone” morphology, which is characteristic of the proximal tubular epithelium, and indicates the high purity of the cell line ¹⁴⁹ (Fig. 2.1). In addition, the cells exhibit very low levels of AGT expression under normal glucose conditions, supporting previous findings that basal levels of AGT expression are lower in the S1 segment than in the other segments under normal conditions ^{45, 46}.

Role of High Glucose on AGT Expression in PTC

During high glucose exposure, AGT protein levels began to increase as early as 3 hours, and were significantly higher after 6 hours (Fig. 3.1A). This high sensitivity of AGT upregulation in response to hyperglycemia supports previous findings that urinary AGT is augmented in patients in the early stages of type 1 ¹¹³ and type 2 DM ¹⁶⁶. p38 mitogen-activated protein kinase is responsible for AGT upregulation by high glucose, but AGT expression was only assessed at 24 hours ¹⁶⁷. Other studies in cultured PTC have also shown AGT upregulation by

indoxyl sulfate ¹⁶⁸, Ang II/interleukin-6 ¹⁵¹, and interferon- γ ¹⁶⁹ after >24 hours in a pathway involving nuclear factor-kappa B and signal transducer and activator of transcription 3 activity. In our experiments, glucose-induced AGT upregulation occurred in a much shorter time period, suggesting that AGT upregulation by high glucose operates using a different intracellular pathway from these other factors reported. Basal AGT protein levels in mPTC sharply declined between 12 and 24 hours, although mRNA and protein levels were still higher in 25 mM glucose compared to 5 mM at 24 hours (Fig. 3.1A and B). Thus, some other factors may be activated to prevent AGT elevation at 24 hours, leading to lower basal AGT expression after 12 hours.

The level of AGT induction also varies between different reports. Hsieh *et al.* demonstrated a 2-fold increase after 24 hours ¹⁷⁰ and prolonged treatments with 25 mM glucose for 2 weeks increased AGT mRNA levels up to 3-fold ^{115, 116}. In type 1 DM rats, a 400-fold increase in urinary AGT after 6 days has been reported ¹¹³, while other groups found a 4-fold increase in AGT mRNA in PTC 2 weeks after diabetes ¹¹⁴. However, AGT regulation in purified S1 cells has been investigated only in this project, therefore, differences in the magnitude of AGT upregulation between experiments are to be expected.

AGT mRNA and protein levels in each proximal tubular segment in type 2 DM rats were compared to non-diabetic rats in a recent study ¹⁷¹. They found that AGT expression was only stimulated in the S3 segment in diabetic rats. Thus, our results demonstrating AGT upregulation by high glucose in S1 cells are in conflict. However, their study examined slowly developing type 2 DM, and the

rats were hyperglycemic for four weeks before AGT was detected. Furthermore, increased intrarenal AGT was shown in type 2 DM rats at 11 weeks ^{111, 172}, and urinary AGT is upregulated within two days after the onset of DM ¹¹³. Therefore, one possibility is that AGT upregulation in the S1 segment could occur initially, and normalize over time.

Effects of Varying Glucose Concentration on AGT Expression

In this study, hyperglycemic conditions enhanced glucose metabolism, indicated by the extracellular acidification rate (ECAR), starting approximately 20 minutes after the addition of high glucose (Fig. 3.3). The increase in extracellular acidification was not different among the three high glucose concentrations chosen (10 mM, 15 mM, or 25 mM), which is consistent with the results that AGT levels were increased after exposure to 15 mM and 25 mM glucose. These levels may exceed the maximum transport capacity of SGLT2. Examining the response in lower glucose levels could reveal a dose-dependent effect on glucose metabolism and AGT expression. Treatment with pyruvate stimulated AGT mRNA expression (Fig. 3.2), suggesting that increased glucose metabolism is involved in AGT augmentation.

ECAR began to decline over the treatment time (Fig. 3.3), which explains the decrease in basal AGT levels as shown in Fig. 3.1. Glucose metabolism is subject to very complex regulation, which might contribute to decreased ECAR. A study by Czajka *et al.* found that treatments of cultured human PTC with 25 mM glucose for 8 days exhibited higher glycolytic activity compared to cells cultured

in 5 mM glucose ¹⁷³, suggesting that high glucose has an overall stimulatory effect on glucose metabolism in the long-term. However, this does not explain the decrease in ECAR at the end of treatment observed in this study. Compensatory mechanisms which lower glucose metabolism and/or H⁺ secretion might be stimulated at the end of experiments, which would neutralize extracellular pH. For example, ATP is an allosteric inhibitor of pyruvate kinase, the final step in glycolysis ¹⁷⁴. It is possible that a sudden increase in ATP generation by high glucose triggers a decrease in metabolic activity and extracellular acidification.

ROS Generation In PTC During High Glucose Treatment

The live-cell images of ROS-induced fluorescence in this study show a clear elevation of ROS generated in high glucose-treated cells compared to normal glucose (Fig. 3.4). Because H₂DCF-DA, the ROS probe used in this study, reacts with several forms of ROS ¹⁵⁸, general oxidative stress is enhanced by high glucose, but the source of ROS is not entirely clear. Hsieh *et al.* reported an 8-fold increase in ROS generation in high glucose-treated PTC that peaked after 10 minutes before declining ¹¹⁵. In this study, increased ROS was still observed at 12 hours of high glucose treatment (Fig. 3.4) accompanied by AGT augmentation (Fig. 3.1A). In contrast, high glucose-induced extracellular acidification was weakened at the end point of 2 hours treatment (Fig 3.3). Thus, in addition to glucose metabolism, there may be other mechanisms facilitating ROS generation in PTC under hyperglycemic conditions. High glucose induces

endoplasmic reticulum stress in PTC leading to intracellular ROS augmentation¹⁷⁵. Accordingly, non-metabolic sources of ROS might help to prolong ROS generation in PTC.

GAPDH is an enzyme involved in glycolysis by mediating the conversion of glyceraldehyde 3-phosphate to D-glycerate 1,3-bisphosphate¹⁷⁶. Although other reports have suggested that GAPDH expression is altered during oxidative stress¹⁷⁷, GAPDH levels were not noticeably affected by high glucose exposure, as shown by western blot using 40 µg protein (Fig. 3.1A). Therefore, GAPDH was used in our western blot data as a housekeeping protein.

AGT upregulation was attenuated by treatment with tempol (Fig. 3.5) in this study. Taurine, another antioxidant, has also been shown to prevent the upregulation of AGT by high glucose in PTC^{115, 116}. Similarly, tempol has been shown to attenuate AGT augmentation in salt-sensitive hypertensive rats¹²⁴. Although tempol significantly attenuated AGT augmentation in this study, AGT expression was still significantly higher in cells treated with 25 mM glucose. There might be a ROS-independent pathway, which at least partially mediates high glucose-induced AGT augmentation in PTC. For example, elevated ATP by glucose metabolism can activate ATPases, leading to the activation of intracellular signaling pathways¹⁷⁸ and consequent AGT upregulation in PTC. Moreover, ATP could stimulate purinergic receptors¹⁷⁹, thus activating signaling pathways as an autocrine or paracrine mechanism. This could help explain why glucose-induced AGT augmentation was not completely prevented by tempol.

Effects of SGLT2 Knockdown on Glucose-Induced AGT Expression

SGLT2 knockdown reduced AGT augmentation during high glucose exposure (Fig. 3.6), indicating that glucose entry via SGLT2 is responsible for AGT upregulation in PTC under hyperglycemic conditions. As introduced in Chapter 1.5, SGLT2 inhibition has been recently utilized as a therapeutic strategy in the treatment of patients with type 2 DM ¹²⁶, and SGLT2 inhibitors are associated with an attenuation of the hypertension in DM ¹³⁸. Because intrarenal RAS activation plays an important role in blood pressure regulation, the suppressing effect of SGLT2 knockdown on AGT upregulation in PTC can help to understand the mechanisms underlying the anti-hypertensive properties of SGLT2 inhibitors.

Detrimental side effects of SGLT2 inhibition have also been reported. Indeed, chronic treatment with SGLT2 inhibitors induces hypoxia, leading to renal acidosis and acute kidney injury ¹⁸⁰, but the evidence for this finding is inconsistent ¹⁸¹. On the other hand, beneficial effects from SGLT2 inhibitors in the development of diabetic nephropathy have also been reported ^{130, 146}, although renoprotection is not universally observed ⁹⁹. In addition to the development of hypertension ⁴¹, inappropriate activation of the intrarenal RAS is a key risk factor in the pathogenesis of diabetic nephropathy ¹⁸², which was demonstrated by showing that RAS blockade delays the onset of kidney injury in patients with type 2 DM ¹⁰¹. Thus, the attenuation of proximal tubular AGT elevation may contribute to the favorable outcomes associated with SGLT2 inhibition.

The suppressing effect of SGLT2 knockdown on high glucose-induced AGT upregulation in cultured PTC was expected and shown in this study. However, there are conflicting studies on the effects of SGLT2 inhibition on urinary AGT levels in rat models of spontaneously developing type 2 DM. Different reports have shown that urinary AGT levels are either lowered¹⁸³ or further increased¹⁸⁴ during SGLT2 inhibition. In the study showing increased urinary AGT levels by SGLT2 inhibitors in type 2 DM, the rats were also on a high-salt diet, which could explain the differing results. Moreover, at 15 and 20 weeks of age, postprandial blood glucose levels were not statistically different among non-diabetic and diabetic rats with or without SGLT2 inhibitors¹⁸⁴, indicating that the rats in all groups did not exhibit hyperglycemia under non-fasting conditions. Therefore, elevated urinary AGT might be induced by other stimuli, but not hyperglycemia in the reported study. Indeed, in the paper reporting decreased urinary AGT by SGLT2 inhibitors in type 2 DM, the rats showed clear hyperglycemia after 12 weeks, which was significantly attenuated by the SGLT2 inhibition¹⁸³. As another possible explanation, inhibition of glucose reabsorption by SGLT2 blockade in the S1 segment would increase glucose levels in the tubular fluid of the S2 and S3 proximal tubular segments, where AGT is highly expressed. The elevated glucose levels could facilitate AGT expression in the later proximal tubule segments in the early phase of treatment. However, the treatment finally lowers blood glucose levels, resulting in the normalization of proximal tubular AGT expression. Namely, SGLT2 blockade could biphasically regulate intrarenal AGT levels, which can explain the

conflicting reports on the effects of SGLT2 inhibitors on intrarenal AGT regulation in DM.

While AGT was upregulated by 15 mM glucose in cells receiving the negative control plasmid (Fig. 3.6), AGT augmentation was smaller than in the other experiments of this project. This could be a result of the electroporation treatment although the shRNA transfection did not alter basal AGT expression levels (5 mM glucose without shRNA versus with shRNA). Since SGLT2 knockdown completely prevented AGT upregulation induced by high glucose, other transporters, such as GLUT2, are unlikely to significantly contribute to the augmentation of AGT. Although GLUT2 is expressed in PTC, and is present on the apical membrane during DM ⁷⁹, it transports glucose via facilitated diffusion. On the other hand, SGLT2 is able to transport glucose up its concentration gradient, suggesting that it can further concentrate intracellular glucose levels ⁷⁸, thus promoting the generation of ROS. Another potential source of intracellular glucose in PTC is gluconeogenesis, which is paradoxically increased during DM ¹⁸⁵. However, a recent study demonstrated that SGLT2 inhibition attenuates the increase in gluconeogenesis during DM ¹⁸⁶. Taken together, an increase in SGLT2-dependent glucose transport is a primary factor leading to AGT upregulation in response to high glucose in S1 PTC.

Effects of Ang II on AGT Expression in PTC

Though Ang II stimulates ROS and intrarenal AGT expression ^{54, 116, 187}, a direct enhancing effect of Ang II or AT1R on glucose-induced AGT expression

was not observed under our experimental conditions (Fig. 4.1 & 4.2). In addition, treatment with an AT1R blocker had no effect on AGT expression, demonstrating that AT1R activation by endogenous Ang II did not contribute to AGT upregulation by high glucose (Fig. 4.1). While increased renin secretion in PTC has been reported during DM ¹⁰⁹, intrarenal Ang II generation may also be increased by elevated renin in the collecting duct ¹⁸⁸, not the proximal tubule in DM. In addition, Ang II treatment did not alter AGT protein levels under normal glucose conditions, and none of the levels had an enhancing effect on AGT expression during high glucose treatment (Fig. 4.2). Ang II may require co-factors present in the diabetic and hypertensive milieu to stimulate AGT expression, such as TGF- β or IL-6. Therefore, *in vitro* experiments in this project failed to show that Ang II directly enhances AGT expression. Previous studies reporting that TGF- β_1 upregulates AGT in PTC ¹⁸⁹, and that TGF- β_1 is upregulated by Ang II during high glucose exposure starting after 24 hours ¹⁰⁵. Thus, extended treatments with Ang II could be required to determine the contribution to ROS and AT1R activation.

Effects of High Glucose and Ang II on SGLT2 Expression

SGLT2 protein levels were not altered by exposure to high glucose or Ang II under our experimental conditions (Fig. 4.3). SGLT2 upregulation has been reported during DM ^{93, 94, 190}, and there is evidence that Ang II stimulates SGLT2 expression during hypertension ¹⁹¹, but this has not been well-established. Other studies in models of both type 1 and 2 DM have reported that SGLT2 expression

is unchanged^{98, 99, 192} or downregulated^{96, 97}. In addition, studies in rabbit PTC have demonstrated a decrease in SGLT2-mediated elevation of intracellular glucose by Ang II¹⁹³ and high glucose¹⁰⁰. Our results are consistent with reports that stimulation with Ang II and hyperglycemia are not sufficient to enhance SGLT2 expression in PTC. Therefore, augmented SGLT2 levels are not required for SGLT2-mediated AGT upregulation by high glucose in PTC. This indicates that DM-associated SGLT2 augmentation is mediated by other factors, and that SGLT2 expression in DM could be sensitive to specific conditions over the course of the disease.

Conclusion

SGLT2 mediates the upregulation of AGT in PTC under hyperglycemic conditions. The response of AGT upregulation to high glucose is highly sensitive compared to other factors reported to stimulate proximal tubular AGT. Furthermore, the high glucose-induced upregulation of AGT does not require extracellular co-factors, which was shown in this study using *in vitro* settings. These results support the previous findings that AGT is augmented in the early stages of DM, before the contribution of other inflammatory stimuli that are elevated in developed kidney injury. High glucose enhances glucose metabolism and increases ROS generation, which is involved in glucose-induced AGT upregulation. In addition, enhanced SGLT2-mediated AGT augmentation does not require enhanced SGLT2 expression in PTC. Taken together, these findings help to elucidate the molecular mechanisms underlying intrarenal RAS activation

during diabetes and suggest novel therapeutic strategies in the treatment of diabetic nephropathy.

CHAPTER 6 – LIST OF REFERENCES

1. Bader M. Tissue renin-angiotensin-aldosterone systems: Targets for pharmacological therapy. *Annu Rev Pharmacol Toxicol*. 2010;50:439-465
2. Sparks MA, Crowley SD, Gurley SB, Mirotso M, Coffman TM. Classical renin-angiotensin system in kidney physiology. *Compr Physiol*. 2014;4:1201-1228
3. Kobori H, Nangaku M, Navar LG, Nishiyama A. The intrarenal renin-angiotensin system: From physiology to the pathobiology of hypertension and kidney disease. *Pharmacol Rev*. 2007;59:251-287
4. Huang XR, Chen WY, Truong LD, Lan HY. Chymase is upregulated in diabetic nephropathy: Implications for an alternative pathway of angiotensin II-mediated diabetic renal and vascular disease. *J Am Soc Nephrol*. 2003;14:1738-1747
5. Allen AM, Zhuo J, Mendelsohn FA. Localization and function of angiotensin AT1 receptors. *Am J Hypertens*. 2000;13:31S-38S
6. Matavelli LC, Siragy HM. At2 receptor activities and pathophysiological implications. *J Cardiovasc Pharmacol*. 2015;65:226-232
7. Matsubara H. Pathophysiological role of angiotensin II type 2 receptor in cardiovascular and renal diseases. *Circ Res*. 1998;83:1182-1191
8. Griendling KK, Rittenhouse SE, Brock TA, Ekstein LS, Gimbrone MA, Jr., Alexander RW. Sustained diacylglycerol formation from inositol phospholipids in angiotensin II-stimulated vascular smooth muscle cells. *J Biol Chem*. 1986;261:5901-5906

9. Griendling KK, Ushio-Fukai M, Lassegue B, Alexander RW. Angiotensin II signaling in vascular smooth muscle. New concepts. *Hypertension*. 1997;29:366-373
10. Liu FY, Cogan MG. Angiotensin II stimulation of hydrogen ion secretion in the rat early proximal tubule. Modes of action, mechanism, and kinetics. *J Clin Invest*. 1988;82:601-607
11. Peti-Peterdi J, Warnock DG, Bell PD. Angiotensin II directly stimulates enac activity in the cortical collecting duct via at(1) receptors. *J Am Soc Nephrol*. 2002;13:1131-1135
12. Aguilera G. Factors controlling steroid biosynthesis in the zona glomerulosa of the adrenal. *J Steroid Biochem Mol Biol*. 1993;45:147-151
13. Bock HA, Hermle M, Brunner FP, Thiel G. Pressure dependent modulation of renin release in isolated perfused glomeruli. *Kidney Int*. 1992;41:275-280
14. Lorenz JN, Weihprecht H, He XR, Skott O, Briggs JP, Schnermann J. Effects of adenosine and angiotensin on macula densa-stimulated renin secretion. *Am J Physiol*. 1993;265:F187-194
15. Gordon RD, Kuchel O, Liddle GW, Island DP. Role of the sympathetic nervous system in regulating renin and aldosterone production in man. *J Clin Invest*. 1967;46:599-605
16. Blair-West JR, Coghlan JP, Denton DA, Funder JW, Scoggins BA, Wright RD. Inhibition of renin secretion by systemic and intrarenal angiotensin infusion. *Am J Physiol*. 1971;220:1309-1315
17. de Champlain J, Genest J, Veyrat R, Boucher R. Factors controlling renin in man. *Trans Assoc Am Physicians*. 1965;78:135-157
18. Corvol P, Jeunemaitre X. Molecular genetics of human hypertension: Role of angiotensinogen. *Endocr Rev*. 1997;18:662-677

19. Cumin F, Le-Nguyen D, Castro B, Menard J, Corvol P. Comparative enzymatic studies of human renin acting on pure natural or synthetic substrates. *Biochim Biophys Acta*. 1987;913:10-19
20. Ito T, Eggena P, Barrett JD, Katz D, Metter J, Sambhi MP. Studies on angiotensinogen of plasma and cerebrospinal fluid in normal and hypertensive human subjects. *Hypertension*. 1980;2:432-436
21. Menard J, el Amrani AI, Savoie F, Bouhnik J. Angiotensinogen: An attractive and underrated participant in hypertension and inflammation. *Hypertension*. 1991;18:705-707
22. Walker WG, Whelton PK, Saito H, Russell RP, Hermann J. Relation between blood pressure and renin, renin substrate, angiotensin II, aldosterone and urinary sodium and potassium in 574 ambulatory subjects. *Hypertension*. 1979;1:287-291
23. Inoue I, Nakajima T, Williams CS, Quackenbush J, Puryear R, Powers M, Cheng T, Ludwig EH, Sharma AM, Hata A, Jeunemaitre X, Lalouel JM. A nucleotide substitution in the promoter of human angiotensinogen is associated with essential hypertension and affects basal transcription in vitro. *J Clin Invest*. 1997;99:1786-1797
24. Deschepper CF. Angiotensinogen: Hormonal regulation and relative importance in the generation of angiotensin II. *Kidney Int*. 1994;46:1561-1563
25. Campbell DJ, Bouhnik J, Menard J, Corvol P. Identity of angiotensinogen precursors of rat brain and liver. *Nature*. 1984;308:206-208
26. Lindpaintner K, Jin M, Wilhelm MJ, Suzuki F, Linz W, Schoelkens BA, Ganten D. Intracardiac generation of angiotensin and its physiologic role. *Circulation*. 1988;77:118-23
27. Engeli S, Negrel R, Sharma AM. Physiology and pathophysiology of the adipose tissue renin-angiotensin system. *Hypertension*. 2000;35:1270-1277

28. Gomez RA, Lynch KR, Chevalier RL, Everett AD, Johns DW, Wilfong N, Peach MJ, Carey RM. Renin and angiotensinogen gene expression and intrarenal renin distribution during ace inhibition. *Am J Physiol.* 1988;254:F900-906
29. Ingelfinger JR, Zuo WM, Fon EA, Ellison KE, Dzau VJ. In situ hybridization evidence for angiotensinogen messenger RNA in the rat proximal tubule. An hypothesis for the intrarenal renin angiotensin system. *J Clin Invest.* 1990;85:417-423
30. Crowley SD, Gurley SB, Herrera MJ, Ruiz P, Griffiths R, Kumar AP, Kim HS, Smithies O, Le TH, Coffman TM. Angiotensin II causes hypertension and cardiac hypertrophy through its receptors in the kidney. *Proc Natl Acad Sci USA.* 2006;103:17985-17990
31. Seikaly MG, Arant BS, Jr., Seney FD, Jr. Endogenous angiotensin concentrations in specific intrarenal fluid compartments of the rat. *J Clin Invest.* 1990;86:1352-1357
32. Navar LG, Lewis L, Hymel A, Braam B, Mitchell KD. Tubular fluid concentrations and kidney contents of angiotensins I and II in anesthetized rats. *J Am Soc Nephrol.* 1994;5:1153-1158
33. Mitchell KD, Navar LG. Enhanced tubuloglomerular feedback during peritubular infusions of angiotensins I and II. *Am J Physiol.* 1988;255:F383-390
34. Bader M, Ganten D. Regulation of renin: New evidence from cultured cells and genetically modified mice. *J Mol Med (Berl).* 2000;78:130-139
35. Moe OW, Ujile K, Star RA, Miller RT, Widell J, Alpern RJ, Henrich WL. Renin expression in renal proximal tubule. *J Clin Invest.* 1993;91:774-779
36. Casarini DE, Boim MA, Stella RC, Krieger-Azzolini MH, Krieger JE, Schor N. Angiotensin I-converting enzyme activity in tubular fluid along the rat nephron. *Am J Physiol.* 1997;272:F405-409
37. Rosivall L, Carmines PK, Navar LG. Effects of renal arterial angiotensin I infusion on glomerular dynamics in sodium replete dogs. *Kidney Int.* 1984;26:263-268

38. Rosivall L, Navar LG. Effects on renal hemodynamics of intra-arterial infusions of angiotensins I and II. *Am J Physiol.* 1983;245:F181-187
39. Inger C, Grima M, Coquard C, Barthelmebs M, Imbs JL. Contribution of angiotensin II internalization to intrarenal angiotensin II levels in rats. *Am J Physiol Renal Physiol.* 2002;283:F1003-1010
40. Li XC, Carretero OA, Navar LG, Zhuo JL. AT1 receptor-mediated accumulation of extracellular angiotensin II in proximal tubule cells: Role of cytoskeleton microtubules and tyrosine phosphatases. *Am J Physiol Renal Physiol.* 2006;291:F375-383
41. Navar LG, Kobori H, Prieto MC, Gonzalez-Villalobos RA. Intratubular renin-angiotensin system in hypertension. *Hypertension.* 2011;57:355-362
42. Yamamoto T, Hayashi K, Matsuda H, Kubota E, Tanaka H, Ogasawara Y, Nakamoto H, Suzuki H, Saruta T, Kajiya F. In vivo visualization of angiotensin II- and tubuloglomerular feedback-mediated renal vasoconstriction. *Kidney Int.* 2001;60:364-369
43. Blantz RC, Konnen KS, Tucker BJ. Angiotensin II effects upon the glomerular microcirculation and ultrafiltration coefficient of the rat. *J Clin Invest.* 1976;57:419-434
44. Rohrwasser A, Morgan T, Dillon HF, Zhao L, Callaway CW, Hillas E, Zhang S, Cheng T, Inagami T, Ward K, Terreros DA, Lalouel JM. Elements of a paracrine tubular renin-angiotensin system along the entire nephron. *Hypertension.* 1999;34:1265-1274
45. Pohl M, Kaminski H, Castrop H, Bader M, Himmerkus N, Bleich M, Bachmann S, Theilig F. Intrarenal renin-angiotensin system revisited: Role of megalin-dependent endocytosis along the proximal nephron. *J Biol Chem.* 2010;285:41935-41946
46. Kamiyama M, Farragut KM, Garner MK, Navar LG, Kobori H. Divergent localization of angiotensinogen mRNA and protein in proximal tubule segments of normal rat kidney. *J Hypertens.* 2012;30:2365-2372

47. Matsusaka T, Nilmura F, Shimizu A, Pastan I, Saito A, Kobori H, Nishiyama A, Ichikawa I. Liver angiotensinogen is the primary source of renal angiotensin II. *J Am Soc Nephrol*. 2012;23:1181-1189
48. Kobori H, Nishiyama A, Harrison-Bernard LM, Navar LG. Urinary angiotensinogen as an indicator of intrarenal angiotensin status in hypertension. *Hypertension*. 2003;41:42-49
49. Nakano D, Kobori H, Burford JL, Gevorgyan H, Seidel S, Hitomi H, Nishiyama A, Peti-Peterdi J. Multiphoton imaging of the glomerular permeability of angiotensinogen. *J Am Soc Nephrol*. 2012;23:1847-1856
50. Ramkumar N, Stuart D, Calquin M, Wang S, Nilmura F, Matsusaka T, Kohan DE. Possible role for nephron-derived angiotensinogen in angiotensin-II dependent hypertension. *Physiol Rep*. 2016;4
51. Kobori H, Nishiyama A, Abe Y, Navar LG. Enhancement of intrarenal angiotensinogen in dahl salt-sensitive rats on high salt diet. *Hypertension*. 2003;41:592-597
52. Kobori H, Harrison-Bernard LM, Navar LG. Enhancement of angiotensinogen expression in angiotensin II-dependent hypertension. *Hypertension*. 2001;37:1329-1335
53. Schunkert H, Ingelfinger JR, Jacob H, Jackson B, Bouyounes B, Dzau VJ. Reciprocal feedback regulation of kidney angiotensinogen and renin mRNA expressions by angiotensin II. *Am J Physiol*. 1992;263:E863-869
54. Kobori H, Prieto-Carrasquero MC, Ozawa Y, Navar LG. At1 receptor mediated augmentation of intrarenal angiotensinogen in angiotensin II-dependent hypertension. *Hypertension*. 2004;43:1126-1132
55. Davisson RL, Ding Y, Stec DE, Catterall JF, Sigmund CD. Novel mechanism of hypertension revealed by cell-specific targeting of human angiotensinogen in transgenic mice. *Physiol Genomics*. 1999;1:3-9

56. Sachetelli S, Liu Q, Zhang SL, Liu F, Hsieh TJ, Brezniceanu ML, Guo DF, Filep JG, Ingelfinger JR, Sigmund CD, Hamet P, Chan JS. Ras blockade decreases blood pressure and proteinuria in transgenic mice overexpressing rat angiotensinogen gene in the kidney. *Kidney Int.* 2006;69:1016-1023
57. Ding Y, Sigmund CD. Androgen-dependent regulation of human angiotensinogen expression in kap-hAGT transgenic mice. *Am J Physiol Renal Physiol.* 2001;280:F54-60
58. Ying J, Stuart D, Hillas E, Gociman BR, Ramkumar N, Lalouel JM, Kohan DE. Overexpression of mouse angiotensinogen in renal proximal tubule causes salt-sensitive hypertension in mice. *Am J Hypertens.* 2012;25:684-689
59. Mather A, Pollock C. Glucose handling by the kidney. *Kidney Int Suppl.* 2011:S1-6
60. Wang Z, Ying Z, Bosy-Westphal A, Zhang J, Schautz B, Later W, Heymsfield SB, Muller MJ. Specific metabolic rates of major organs and tissues across adulthood: Evaluation by mechanistic model of resting energy expenditure. *Am J Clin Nutr.* 2010;92:1369-1377
61. Abdul-Ghani MA, DeFronzo RA, Norton L. Novel hypothesis to explain why SGLT2 inhibitors inhibit only 30-50% of filtered glucose load in humans. *Diabetes.* 2013;62:3324-3328
62. Polidori D, Sha S, Mudaliar S, Ciaraldi TP, Ghosh A, Vaccaro N, Farrell K, Rothenberg P, Henry RR. Canagliflozin lowers postprandial glucose and insulin by delaying intestinal glucose absorption in addition to increasing urinary glucose excretion: Results of a randomized, placebo-controlled study. *Diabetes Care.* 2013;36:2154-2161
63. Vallon V, Platt KA, Cunard R, Schroth J, Whaley J, Thomson SC, Koepsell H, Rieg T. SGLT2 mediates glucose reabsorption in the early proximal tubule. *J Am Soc Nephrol.* 2011;22:104-112
64. Frohnert PP, Hohmann B, Zwiebel R, Baumann K. Free flow micropuncture studies of glucose transport in the rat nephron. *Pflugers Arch.* 1970;315:66-85

65. Baines AD. Effect of extracellular fluid volume expansion on maximum glucose reabsorption rate and glomerular tubular balance in single rat nephrons. *J Clin Invest.* 1971;50:2414-2425
66. Tune BM, Burg MB. Glucose transport by proximal renal tubules. *Am J Physiol.* 1971;221:580-585
67. Barfuss DW, Schafer JA. Differences in active and passive glucose transport along the proximal nephron. *Am J Physiol.* 1981;241:F322-332
68. Turner RJ, Moran A. Heterogeneity of sodium-dependent D-glucose transport sites along the proximal tubule: Evidence from vesicle studies. *Am J Physiol.* 1982;242:F406-414
69. DeFronzo RA, Norton L, Abdul-Ghani M. Renal, metabolic and cardiovascular considerations of SGLT2 inhibition. *Nat Rev Nephrol.* 2017;13:11-26
70. Wright EM, Loo DD, Hirayama BA. Biology of human sodium glucose transporters. *Physiol Rev.* 2011;91:733-794
71. Hediger MA, Rhoads DB. Molecular physiology of sodium-glucose cotransporters. *Physiol Rev.* 1994;74:993-1026
72. Vallon V. The proximal tubule in the pathophysiology of the diabetic kidney. *Am J Physiol Regul Integr Comp Physiol.* 2011;300:R1009-1022
73. Sacktor B. Sodium-coupled hexose transport. *Kidney Int.* 1989;36:342-350
74. Wright EM, Loo DD, Hirayama BA, Turk E. Surprising versatility of Na⁺-glucose cotransporters: Slc5. *Physiology (Bethesda).* 2004;19:370-376
75. Santer R, Calado J. Familial renal glucosuria and SGLT2: From a mendelian trait to a therapeutic target. *Clin J Am Soc Nephrol.* 2010;5:133-141

76. Yoshida A, Takata K, Kasahara T, Aoyagi T, Saito S, Hirano H. Immunohistochemical localization of na(+)-dependent glucose transporter in the rat digestive tract. *Histochem J*. 1995;27:420-426
77. Vrhovac I, Balen Eror D, Klessen D, Burger C, Breljak D, Kraus O, Radovic N, Jadrijevic S, Aleksic I, Walles T, Sauvans C, Sabolic I, Koepsell H. Localizations of na(+)-d-glucose cotransporters sglt1 and SGLT2 in human kidney and of sglt1 in human small intestine, liver, lung, and heart. *Pflugers Arch*. 2015;467:1881-1898
78. Dominguez JH, Song B, Maianu L, Garvey WT, Qulali M. Gene expression of epithelial glucose transporters: The role of diabetes mellitus. *J Am Soc Nephrol*. 1994;5:S29-36
79. Leturque A, Brot-Laroche E, Le Gall M. GLUT2 mutations, translocation, and receptor function in diet sugar managing. *Am J Physiol Endocrinol Metab*. 2009;296:E985-992
80. Marks J, Carvou NJ, Debnam ES, Srai SK, Unwin RJ. Diabetes increases facilitative glucose uptake and GLUT2 expression at the rat proximal tubule brush border membrane. *J Physiol*. 2003;553:137-145
81. Tuttle KR, Bakris GL, Bilous RW, Chiang JL, de Boer IH, Goldstein-Fuchs J, Hirsch IB, Kalantar-Zadeh K, Narva AS, Navaneethan SD, Neumiller JJ, Patel UD, Ratner RE, Whaley-Connell AT, Molitch ME. Diabetic kidney disease: A report from an ada consensus conference. *Am J Kidney Dis*. 2014;64:510-533
82. Guariguata L, Whiting DR, Hambleton I, Beagley J, Linnenkamp U, Shaw JE. Global estimates of diabetes prevalence for 2013 and projections for 2035. *Diabetes Res Clin Pract*. 2014;103:137-149
83. Us renal data system 2016 annual data report: Epidemiology of kidney disease in the united states. *Am J Kidney Dis*. 2017;69:A4
84. Shlipak M. Diabetic nephropathy: Preventing progression. *BMJ Clin Evid*. 2010;2010

85. Mora-Fernandez C, Dominguez-Pimentel V, de Fuentes MM, Gorriz JL, Martinez-Castelao A, Navarro-Gonzalez JF. Diabetic kidney disease: From physiology to therapeutics. *J Physiol*. 2014;592:3997-4012
86. Gross JL, de Azevedo MJ, Silveiro SP, Canani LH, Caramori ML, Zelmanovitz T. Diabetic nephropathy: Diagnosis, prevention, and treatment. *Diabetes Care*. 2005;28:164-176
87. Kumar D, Robertson S, Burns KD. Evidence of apoptosis in human diabetic kidney. *Mol Cell Biochem*. 2004;259:67-70
88. Mogensen CE, Christensen CK. Predicting diabetic nephropathy in insulin-dependent patients. *N Engl J Med*. 1984;311:89-93
89. Rigalleau V, Garcia M, Lasseur C, Laurent F, Montaudon M, Raffaitin C, Barthe N, Beauvieux MC, Vendrely B, Chauveau P, Combe C, Gin H. Large kidneys predict poor renal outcome in subjects with diabetes and chronic kidney disease. *BMC Nephrol*. 2010;11:3
90. Zerbini G, Bonfanti R, Meschi F, Bognetti E, Paesano PL, Gianolli L, Querques M, Maestroni A, Calori G, Del Maschio A, Fazio F, Luzi L, Chiumello G. Persistent renal hypertrophy and faster decline of glomerular filtration rate precede the development of microalbuminuria in type 1 diabetes. *Diabetes*. 2006;55:2620-2625
91. Bank N, Aynedjian HS. Progressive increases in luminal glucose stimulate proximal sodium absorption in normal and diabetic rats. *J Clin Invest*. 1990;86:309-316
92. Vallon V, Richter K, Blantz RC, Thomson S, Osswald H. Glomerular hyperfiltration in experimental diabetes mellitus: Potential role of tubular reabsorption. *J Am Soc Nephrol*. 1999;10:2569-2576
93. Vestri S, Okamoto MM, de Freitas HS, Aparecida Dos Santos R, Nunes MT, Morimatsu M, Heimann JC, Machado UF. Changes in sodium or glucose filtration rate modulate expression of glucose transporters in renal proximal tubular cells of rat. *J Membr Biol*. 2001;182:105-112

94. Tabatabai NM, Sharma M, Blumenthal SS, Petering DH. Enhanced expressions of sodium-glucose cotransporters in the kidneys of diabetic zucker rats. *Diabetes Res Clin Pract.* 2009;83:e27-30
95. Rahmoune H, Thompson PW, Ward JM, Smith CD, Hong G, Brown J. Glucose transporters in human renal proximal tubular cells isolated from the urine of patients with non-insulin-dependent diabetes. *Diabetes.* 2005;54:3427-3434
96. Vallon V, Rose M, Gerasimova M, Satriano J, Platt KA, Koepsell H, Cunard R, Sharma K, Thomson SC, Rieg T. Knockout of na-glucose transporter SGLT2 attenuates hyperglycemia and glomerular hyperfiltration but not kidney growth or injury in diabetes mellitus. *Am J Physiol Renal Physiol.* 2013;304:F156-167
97. Albertoni Borghese MF, Majowicz MP, Ortiz MC, Passalacqua Mdel R, Sterin Speziale NB, Vidal NA. Expression and activity of SGLT2 in diabetes induced by streptozotocin: Relationship with the lipid environment. *Nephron Physiol.* 2009;112:p45-52
98. Adachi T, Yasuda K, Okamoto Y, Shihara N, Oku A, Ueta K, Kitamura K, Saito A, Iwakura I, Yamada Y, Yano H, Seino Y, Tsuda K. T-1095, a renal Na⁺-glucose transporter inhibitor, improves hyperglycemia in streptozotocin-induced diabetic rats. *Metabolism.* 2000;49:990-995
99. Gallo LA, Ward MS, Fotheringham AK, Zhuang A, Borg DJ, Flemming NB, Harvie BM, Kinneally TL, Yeh SM, McCarthy DA, Koepsell H, Vallon V, Pollock C, Panchapakesan U, Forbes JM. Once daily administration of the SGLT2 inhibitor, empagliflozin, attenuates markers of renal fibrosis without improving albuminuria in diabetic db/db mice. *Sci Rep.* 2016;6:26428
100. Han HJ, Choi HJ, Park SH. High glucose inhibits glucose uptake in renal proximal tubule cells by oxidative stress and protein kinase c. *Kidney Int.* 2000;57:918-926
101. Andersen S, Tarnow L, Rossing P, Hansen BV, Parving HH. Renoprotective effects of angiotensin II receptor blockade in type 1 diabetic patients with diabetic nephropathy. *Kidney Int.* 2000;57:601-606
102. Lewis EJ, Lewis JB. Treatment of diabetic nephropathy with angiotensin II receptor antagonist. *Clin Exp Nephrol.* 2003;7:1-8

103. Sarafidis PA, Stafylas PC, Kanaki AI, Lasaridis AN. Effects of renin-angiotensin system blockers on renal outcomes and all-cause mortality in patients with diabetic nephropathy: An updated meta-analysis. *Am J Hypertens*. 2008;21:922-929
104. Ogawa S, Kobori H, Ohashi N, Urushihara M, Nishiyama A, Mori T, Ishizuka T, Nako K, Ito S. Angiotensin II type 1 receptor blockers reduce urinary angiotensinogen excretion and the levels of urinary markers of oxidative stress and inflammation in patients with type 2 diabetic nephropathy. *Biomarker insights*. 2009;4:97-102
105. Wolf G, Mueller E, Stahl RA, Ziyadeh FN. Angiotensin II-induced hypertrophy of cultured murine proximal tubular cells is mediated by endogenous transforming growth factor-beta. *J Clin Invest*. 1993;92:1366-1372
106. Wolf G, Neilson EG. Angiotensin II induces cellular hypertrophy in cultured murine proximal tubular cells. *Am J Physiol*. 1990;259:F768-777
107. Bhaskaran M, Reddy K, Radhakrishanan N, Franki N, Ding G, Singhal PC. Angiotensin II induces apoptosis in renal proximal tubular cells. *Am J Physiol Renal Physiol*. 2003;284:F955-965
108. Kelly DJ, Cox AJ, Tolcos M, Cooper ME, Wilkinson-Berka JL, Gilbert RE. Attenuation of tubular apoptosis by blockade of the renin-angiotensin system in diabetic ren-2 rats. *Kidney Int*. 2002;61:31-39
109. Zimpelmann J, Kumar D, Levine DZ, Wehbi G, Imig JD, Navar LG, Burns KD. Early diabetes mellitus stimulates proximal tubule renin mRNA expression in the rat. *Kidney Int*. 2000;58:2320-2330
110. Suzaki Y, Ozawa Y, Kobori H. Intrarenal oxidative stress and augmented angiotensinogen are precedent to renal injury in Zucker diabetic fatty rats. *Int J Biol Sci*. 2006;3:40-46
111. Nagai Y, Yao L, Kobori H, Miyata K, Ozawa Y, Miyatake A, Yukimura T, Shokoji T, Kimura S, Kiyomoto H, Kohno M, Abe Y, Nishiyama A. Temporary angiotensin II blockade at the prediabetic stage attenuates the development of renal injury in type 2 diabetic rats. *J Am Soc Nephrol*. 2005;16:703-711

112. Saito T, Urushihara M, Kotani Y, Kagami S, Kobori H. Increased urinary angiotensinogen is precedent to increased urinary albumin in patients with type 1 diabetes. *Am J Med Sci.* 2009;338:478-480
113. Kamiyama M, Zsombok A, Kobori H. Urinary angiotensinogen as a novel early biomarker of intrarenal renin-angiotensin system activation in experimental type 1 diabetes. *J Pharmacol Sci.* 2012;119:314-323
114. Brezniceanu ML, Liu F, Wei CC, Tran S, Sachetelli S, Zhang SL, Guo DF, Filep JG, Ingelfinger JR, Chan JS. Catalase overexpression attenuates angiotensinogen expression and apoptosis in diabetic mice. *Kidney Int.* 2007;71:912-923
115. Hsieh TJ, Zhang SL, Filep JG, Tang SS, Ingelfinger JR, Chan JS. High glucose stimulates angiotensinogen gene expression via reactive oxygen species generation in rat kidney proximal tubular cells. *Endocrinology.* 2002;143:2975-2985
116. Hsieh TJ, Fustier P, Wei CC, Zhang SL, Filep JG, Tang SS, Ingelfinger JR, Fantus IG, Hamet P, Chan JS. Reactive oxygen species blockade and action of insulin on expression of angiotensinogen gene in proximal tubular cells. *J Endocrinol.* 2004;183:535-550
117. Turrens JF, Boveris A. Generation of superoxide anion by the NADH dehydrogenase of bovine heart mitochondria. *Biochemical J.* 1980;191:421-427
118. Murphy MP. How mitochondria produce reactive oxygen species. *Biochem J.* 2009;417:1-13
119. Turrens JF. Mitochondrial formation of reactive oxygen species. *J Physiol.* 2003;552:335-344
120. Baughman JM, Mootha VK. Buffering mitochondrial DNA variation. *Nat Genet.* 2006;38:1232-1233
121. Munusamy S, MacMillan-Crow LA. Mitochondrial superoxide plays a crucial role in the development of mitochondrial dysfunction during high glucose exposure in rat renal proximal tubular cells. *Free Radic Biol Med.* 2009;46:1149-1157

122. Seshiah PN, Weber DS, Rocic P, Valppu L, Taniyama Y, Griendling KK. Angiotensin II stimulation of NAD(P)H oxidase activity: Upstream mediators. *Circ Res*. 2002;91:406-413
123. Hannken T, Schroeder R, Zahner G, Stahl RA, Wolf G. Reactive oxygen species stimulate p44/42 mitogen-activated protein kinase and induce p27(kip1): Role in angiotensin II-mediated hypertrophy of proximal tubular cells. *J Am Soc Nephrol*. 2000;11:1387-1397
124. Kobori H, Nishiyama A. Effects of tempol on renal angiotensinogen production in Dahl salt-sensitive rats. *Biochem Biophys Res Commun*. 2004;315:746-750
125. Liu F, Wei CC, Wu SJ, Chenier I, Zhang SL, Filep JG, Ingelfinger JR, Chan JS. Apocynin attenuates tubular apoptosis and tubulointerstitial fibrosis in transgenic mice independent of hypertension. *Kidney Int*. 2009;75:156-166
126. Chao EC, Henry RR. SGLT2 inhibition--a novel strategy for diabetes treatment. *Nature reviews. Drug discovery*. 2010;9:551-559
127. Abdul-Ghani MA, Norton L, DeFronzo RA. Efficacy and safety of SGLT2 inhibitors in the treatment of type 2 diabetes mellitus. *Curr Diab Rep*. 2012;12:230-238
128. Kahn BB, Shulman GI, DeFronzo RA, Cushman SW, Rossetti L. Normalization of blood glucose in diabetic rats with phlorizin treatment reverses insulin-resistant glucose transport in adipose cells without restoring glucose transporter gene expression. *J Clin Invest*. 1991;87:561-570
129. Oliva RV, Bakris GL. Blood pressure effects of sodium-glucose co-transport 2 (SGLT2) inhibitors. *J Am Soc Hypertens*. 2014;8:330-339
130. Cherney DZ, Perkins BA, Soleymanlou N, Maione M, Lai V, Lee A, Fagan NM, Woerle HJ, Johansen OE, Broedl UC, von Eynatten M. Renal hemodynamic effect of sodium-glucose cotransporter 2 inhibition in patients with type 1 diabetes mellitus. *Circulation*. 2014;129:587-597

131. Gosch C, Halbwirth H, Stich K. Phloridzin: Biosynthesis, distribution and physiological relevance in plants. *Phytochemistry*. 2010;71:838-843
132. Goldring W, Welsh C. The effects on renal activity of the oral administration of phlorizin in man. *J Clin Invest*. 1934;13:749-752
133. Harsing L, Fonyodi S, Kabat M, Kover G. [effects of phlorhizin and mercurial diuretics on renal hemodynamics]. *Kiserl Orvostud*. 1957;9:337-344
134. Washburn WN. Development of the renal glucose reabsorption inhibitors: A new mechanism for the pharmacotherapy of diabetes mellitus type 2. *J Med Chem*. 2009;52:1785-1794
135. Hummel CS, Lu C, Liu J, Ghezzi C, Hirayama BA, Loo DD, Kepe V, Barrio JR, Wright EM. Structural selectivity of human SGLT inhibitors. *Am J Physiol Cell Physiol*. 2012;302:C373-382
136. Abdul-Ghani MA, Norton L, DeFronzo RA. Role of sodium-glucose cotransporter 2 (SGLT 2) inhibitors in the treatment of type 2 diabetes. *Endocr Rev*. 2011;32:515-531
137. DeFronzo RA, Hompesch M, Kasichayanula S, Liu X, Hong Y, Pfister M, Morrow LA, Leslie BR, Boulton DW, Ching A, LaCreta FP, Griffen SC. Characterization of renal glucose reabsorption in response to dapagliflozin in healthy subjects and subjects with type 2 diabetes. *Diabetes Care*. 2013;36:3169-3176
138. Baker WL, Smyth LR, Riche DM, Bourret EM, Chamberlin KW, White WB. Effects of sodium-glucose co-transporter 2 inhibitors on blood pressure: A systematic review and meta-analysis. *J Am Soc Hypertens*. 2014;8:262-275 e269
139. Komoroski B, Vachharajani N, Boulton D, Kornhauser D, Geraldles M, Li L, Pfister M. Dapagliflozin, a novel SGLT2 inhibitor, induces dose-dependent glucosuria in healthy subjects. *Clin Pharmacol Ther*. 2009;85:520-526

140. Sha S, Devineni D, Ghosh A, Polidori D, Chien S, Wexler D, Shalayda K, Demarest K, Rothenberg P. Canagliflozin, a novel inhibitor of sodium glucose co-transporter 2, dose dependently reduces calculated renal threshold for glucose excretion and increases urinary glucose excretion in healthy subjects. *Diabetes Obes Metab*. 2011;13:669-672
141. Thomson SC, Rieg T, Miracle C, Mansoury H, Whaley J, Vallon V, Singh P. Acute and chronic effects of SGLT2 blockade on glomerular and tubular function in the early diabetic rat. *Am J Physiol Regul Integr Comp Physiol*. 2012;302:R75-83
142. Stanton RC. Sodium glucose transport 2 (SGLT2) inhibition decreases glomerular hyperfiltration: Is there a role for SGLT2 inhibitors in diabetic kidney disease? *Circulation*. 2014;129:542-544
143. Devineni D, Curtin CR, Polidori D, Gutierrez MJ, Murphy J, Rusch S, Rothenberg PL. Pharmacokinetics and pharmacodynamics of canagliflozin, a sodium glucose co-transporter 2 inhibitor, in subjects with type 2 diabetes mellitus. *J Clin Pharmacol*. 2013;53:601-610
144. Gilbert RE. Sodium-glucose linked transporter-2 inhibitors: Potential for renoprotection beyond blood glucose lowering? *Kidney Int*. 2014;86:693-700
145. Arakawa K, Ishihara T, Oku A, Nawano M, Ueta K, Kitamura K, Matsumoto M, Saito A. Improved diabetic syndrome in c57bl/ksj-db/db mice by oral administration of the Na(+)-glucose cotransporter inhibitor T-1095. *Br J Pharmacol*. 2001;132:578-586
146. Kojima N, Williams JM, Takahashi T, Miyata N, Roman RJ. Effects of a new SGLT2 inhibitor, luseogliflozin, on diabetic nephropathy in T2DN rats. *J Pharmacol Exp Ther*. 2013;345:464-472
147. Navar LG, Harrison-Bernard LM, Imig JD, Wang CT, Cervenka L, Mitchell KD. Intrarenal angiotensin II generation and renal effects of at1 receptor blockade. *J Am Soc Nephrol*. 1999;10 Suppl 12:S266-272
148. Kern G, Flucher BE. Localization of transgenes and genotyping of h-2kb-tsa58 transgenic mice. *Biotechniques*. 2005;38:38, 40, 42

149. Hopfer U, Jacobberger JW, Gruenert DC, Eckert RL, Jat PS, Whitsett JA. Immortalization of epithelial cells. *Am J Physiol*. 1996;270:C1-11
150. Woost PG, Kolb RJ, Finesilver M, Mackraj I, Imboden H, Coffman TM, Hopfer U. Strategy for the development of a matched set of transport-competent, angiotensin receptor-deficient proximal tubule cell lines. *In Vitro Cell Dev Biol Anim*. 2006;42:189-200
151. Satou R, Gonzalez-Villalobos RA, Miyata K, Ohashi N, Katsurada A, Navar LG, Kobori H. Costimulation with angiotensin II and interleukin 6 augments angiotensinogen expression in cultured human renal proximal tubular cells. *Am J Physiol Renal Physiol*. 2008;295:F283-289
152. Gariboldi MB, Lucchi S, Caserini C, Supino R, Oliva C, Monti E. Antiproliferative effect of the piperidine nitroxide tempol on neoplastic and nonneoplastic mammalian cell lines. *Free Radic Biol Med*. 1998;24:913-923
153. Engelgau MM, Narayan KM, Herman WH. Screening for type 2 diabetes. *Diabetes Care*. 2000;23:1563-1580
154. Freeman WM, Walker SJ, Vrana KE. Quantitative rt-pcr: Pitfalls and potential. *Biotechniques*. 1999;26:112-122, 124-115
155. Holland PM, Abramson RD, Watson R, Gelfand DH. Detection of specific polymerase chain reaction product by utilizing the 5'----3' exonuclease activity of thermus aquaticus DNA polymerase. *Proc Natl Acad Sci USA*. 1991;88:7276-7280
156. Gelmini S, Orlando C, Sestini R, Vona G, Pinzani P, Ruocco L, Pazzagli M. Quantitative polymerase chain reaction-based homogeneous assay with fluorogenic probes to measure c-erbB-2 oncogene amplification. *Clin Chem*. 1997;43:752-758
157. Wang H, Joseph JA. Quantifying cellular oxidative stress by dichlorofluorescein assay using microplate reader. *Free Radic Biol Med*. 1999;27:612-616

158. LeBel CP, Ischiropoulos H, Bondy SC. Evaluation of the probe 2',7'-dichlorofluorescein as an indicator of reactive oxygen species formation and oxidative stress. *Chem Res Toxicol*. 1992;5:227-231
159. Ryoo IG, Shin DH, Kang KS, Kwak MK. Involvement of nrf2-gsh signaling in TGFbeta1-stimulated epithelial-to-mesenchymal transition changes in rat renal tubular cells. *Arch Pharm Res*. 2015;38:272-281
160. Dranka BP, Benavides GA, Diers AR, Giordano S, Zelickson BR, Reily C, Zou L, Chatham JC, Hill BG, Zhang J, Landar A, Darley-Usmar VM. Assessing bioenergetic function in response to oxidative stress by metabolic profiling. *Free Radic Biol Med*. 2011;51:1621-1635
161. Wu M, Neilson A, Swift AL, Moran R, Tamagnine J, Parslow D, Armistead S, Lemire K, Orrell J, Teich J, Chomicz S, Ferrick DA. Multiparameter metabolic analysis reveals a close link between attenuated mitochondrial bioenergetic function and enhanced glycolysis dependency in human tumor cells. *Am J Physiol Cell Physiol*. 2007;292:C125-136
162. Xiang S, Fruehauf J, Li CJ. Short hairpin rna-expressing bacteria elicit RNA interference in mammals. *Nat Biotechnol*. 2006;24:697-702
163. Paddison PJ, Caudy AA, Bernstein E, Hannon GJ, Conklin DS. Short hairpin rnas (shrnas) induce sequence-specific silencing in mammalian cells. *Genes Dev*. 2002;16:948-958
164. Freeman SA, Wang MA, Weaver JC. Theory of electroporation of planar bilayer membranes: Predictions of the aqueous area, change in capacitance, and pore-pore separation. *Biophys J*. 1994;67:42-56
165. Tsong TY. Electroporation of cell membranes. *Biophys J*. 1991;60:297-306
166. Zhuang Z, Bai Q, A L, Liang Y, Zheng D, Wang Y. Increased urinary angiotensinogen precedes the onset of albuminuria in normotensive type 2 diabetic patients. *Int J Clin Exp Pathol*. 2015;8:11464-11469

167. Zhang SL, Tang SS, Chen X, Filep JG, Ingelfinger JR, Chan JS. High levels of glucose stimulate angiotensinogen gene expression via the p38 mitogen-activated protein kinase pathway in rat kidney proximal tubular cells. *Endocrinology*. 2000;141:4637-4646
168. Shimizu H, Saito S, Higashiyama Y, Nishijima F, Niwa T. Creb, nf-kappab, and nadph oxidase coordinately upregulate indoxyl sulfate-induced angiotensinogen expression in proximal tubular cells. *Am J Physiol Cell Physiol*. 2013;304:C685-692
169. Satou R, Miyata K, Gonzalez-Villalobos RA, Ingelfinger JR, Navar LG, Kobori H. Interferon-gamma biphasically regulates angiotensinogen expression via a jak-stat pathway and suppressor of cytokine signaling 1 (SOCS1) in renal proximal tubular cells. *FASEB J*. 2012;26:1821-1830
170. Ingelfinger JR, Jung F, Diamant D, Haveran L, Lee E, Brem A, Tang SS. Rat proximal tubule cell line transformed with origin-defective sv40 DNA: Autocrine ang II feedback. *Am J Physiol*. 1999;276:F218-227
171. Kamiyama M, Garner MK, Farragut KM, Sofue T, Hara T, Morikawa T, Konishi Y, Imanishi M, Nishiyama A, Kobori H. Detailed localization of augmented angiotensinogen mRNA and protein in proximal tubule segments of diabetic kidneys in rats and humans. *Int J Biol Sci*. 2014;10:530-542
172. Fan YY, Kobori H, Nakano D, Hitomi H, Mori H, Masaki T, Sun YX, Zhi N, Zhang L, Huang W, Zhu B, Li P, Nishiyama A. Aberrant activation of the intrarenal renin-angiotensin system in the developing kidneys of type 2 diabetic rats. *Horm Metab Res*. 2013;45:338-343
173. Czajka A, Malik AN. Hyperglycemia induced damage to mitochondrial respiration in renal mesangial and tubular cells: Implications for diabetic nephropathy. *Redox Biol*. 2016;10:100-107
174. Carbonell J, Feliu JE, Marco R, Sols A. Pyruvate kinase. Classes of regulatory isoenzymes in mammalian tissues. *Eur J Biochem*. 1973;37:148-156
175. Liu G, Sun Y, Li Z, Song T, Wang H, Zhang Y, Ge Z. Apoptosis induced by endoplasmic reticulum stress involved in diabetic kidney disease. *Biochem Biophys Res Commun*. 2008;370:651-656

176. Tarze A, Deniaud A, Le Bras M, Maillier E, Molle D, Larochette N, Zamzami N, Jan G, Kroemer G, Brenner C. GAPDH, a novel regulator of the pro-apoptotic mitochondrial membrane permeabilization. *Oncogene*. 2007;26:2606-2620
177. Bereta J, Bereta M. Stimulation of glyceraldehyde-3-phosphate dehydrogenase mRNA levels by endogenous nitric oxide in cytokine-activated endothelium. *Biochem Biophys Res Commun*. 1995;217:363-369
178. Bertorello A, Aperia A. Na⁺-K⁺-ATPase is an effector protein for protein kinase c in renal proximal tubule cells. *Am J Physiol*. 1989;256:F370-373
179. Unwin RJ, Bailey MA, Burnstock G. Purinergic signaling along the renal tubule: The current state of play. *News Physiol Sci*. 2003;18:237-241
180. Hahn K, Ejaz AA, Kanbay M, Lanaspa MA, Johnson RJ. Acute kidney injury from SGLT2 inhibitors: Potential mechanisms. *Nat Rev Nephrol*. 2016;12:711-712
181. Zinman B, Lachin JM, Inzucchi SE. Empagliflozin, cardiovascular outcomes, and mortality in type 2 diabetes. *N Engl J Med*. 2016;374:1094
182. Kobori H, Kamiyama M, Harrison-Bernard LM, Navar LG. Cardinal role of the intrarenal renin-angiotensin system in the pathogenesis of diabetic nephropathy. *J Investig Med*. 2013;61:256-264
183. Shin SJ, Chung S, Kim SJ, Lee EM, Yoo YH, Kim JW, Ahn YB, Kim ES, Moon SD, Kim MJ, Ko SH. Effect of sodium-glucose co-transporter 2 inhibitor, dapagliflozin, on renal renin-angiotensin system in an animal model of type 2 diabetes. *PloS one*. 2016;11:e0165703
184. Takeshige Y, Fujisawa Y, Rahman A, Kittikulsuth W, Nakano D, Mori H, Masaki T, Ohmori K, Kohno M, Ogata H, Nishiyama A. A sodium-glucose co-transporter 2 inhibitor empagliflozin prevents abnormality of circadian rhythm of blood pressure in salt-treated obese rats. *Hypertens Res*. 2016;39:415-422

185. Meyer C, Woerle HJ, Dostou JM, Welle SL, Gerich JE. Abnormal renal, hepatic, and muscle glucose metabolism following glucose ingestion in type 2 diabetes. *Am J Physiol Endocrinol Metab.* 2004;287:E1049-1056
186. Vallon V, Gerasimova M, Rose MA, Masuda T, Satriano J, Mayoux E, Koepsell H, Thomson SC, Rieg T. SGLT2 inhibitor empagliflozin reduces renal growth and albuminuria in proportion to hyperglycemia and prevents glomerular hyperfiltration in diabetic akita mice. *Am J Physiol Renal Physiol.* 2014;306:F194-204
187. Haugen EN, Croatt AJ, Nath KA. Angiotensin II induces renal oxidant stress in vivo and heme oxygenase-1 in vivo and in vitro. *Kidney Int.* 2000;58:144-152
188. Kang JJ, Toma I, Sipos A, Meer EJ, Vargas SL, Peti-Peterdi J. The collecting duct is the major source of prorenin in diabetes. *Hypertension.* 2008;51:1597-1604
189. Brezniceanu ML, Wei CC, Zhang SL, Hsieh TJ, Guo DF, Hebert MJ, Ingelfinger JR, Filep JG, Chan JS. Transforming growth factor-beta 1 stimulates angiotensinogen gene expression in kidney proximal tubular cells. *Kidney Int.* 2006;69:1977-1985
190. Osorio H, Bautista R, Rios A, Franco M, Santamaria J, Escalante B. Effect of treatment with losartan on salt sensitivity and SGLT2 expression in hypertensive diabetic rats. *Diabetes Res Clin Pract.* 2009;86:e46-49
191. Bautista R, Manning R, Martinez F, Avila-Casado Mdel C, Soto V, Medina A, Escalante B. Angiotensin II-dependent increased expression of Na⁺-glucose cotransporter in hypertension. *Am J Physiol Renal Physiol.* 2004;286:F127-133
192. Kamran M, Peterson RG, Dominguez JH. Overexpression of GLUT2 gene in renal proximal tubules of diabetic zucker rats. *J Am Soc Nephrol.* 1997;8:943-948
193. Han HJ, Park SH, Lee YJ. Signaling cascade of ang II-induced inhibition of alpha-mg uptake in renal proximal tubule cells. *Am J Physiol Renal Physiol.* 2004;286:F634-642

BIOGRAPHY

Michael Winthers Cypress was born in Nashville, Tennessee on May 21, 1988. At an early age, he developed an interest in biology and mathematics, which he cultivated at University School of Nashville. Michael attended University of Rochester in Rochester, New York graduating with a B.S. in Biological Sciences concentrating in Molecular Genetics, and a B.S. in Mathematics. After graduation, Michael worked for one year as a laboratory technician at the University of Rochester Medical Center. In 2011, Michael attended graduate school at Tulane University in New Orleans, Louisiana to pursue a Ph.D. in Cell and Molecular Biology. Upon graduating in the spring of 2017, Michael plans to pursue a career in teaching and research.

Recognizing that we have the kind of internal environment we have because we have the kind of kidneys we have, we must acknowledge that our kidneys constitute the major foundation of our physiological freedom. Only because they work the way they do has it become possible for us to have bones, muscles, glands, and brains. Superficially, it might be said that the function of the kidney is to make urine; but in a more considered view one can say that the kidneys make the stuff of philosophy itself.

-- Homer Smith